Calhoun: The NPS Institutional Archive

DSpace Repository

Theses and Dissertations 1. Thesis and Dissertation Collection, all items

1975-06

# Digital control of a shipboard turbogenerator.

Hatcher, William Lloyd III

Northwestern University

http://hdl.handle.net/10945/20822

This publication is a work of the U.S. Government as defined in Title 17, United States Code, Section 101. Copyright protection is not available for this work in the United States.

*Downloaded from NPS Archive: Calhoun*

Calhoun is the Naval Postgraduate School's public access digital repository for research materials and institutional publications created by the NPS community. Calhoun is named for Professor of Mathematics Guy K. Calhoun, NPS's first appointed -- and published -- scholarly author.

Dudley Knox Library / Naval Postgraduate School
411 Dyer Road / 1 University Circle
Monterey, California USA 93943

http://www.nps.edu/library

# DIGITAL CONTROL OF A SHIPBOARD TURBOGENERATOR

William Lloyd Hatcher

DUDLEY KNOX LIBRARY
NAVAL POSTGRADUATE SCHOOL
MONTEREY, CALIFORNIA 93940

NORTHWESTERN UNIVERSITY

# DIGITAL CONTROL OF A SHIPBOARD TURBOGENERATOR

A THESIS

SUBMITTED TO THE GRADUATE SCHOOL

IN PARTIAL FULFILLMENT OF THE REQUIREMENTS

for the degree

MASTER OF SCIENCE

Field of Electrical Engineering

By

William Lloyd Hatcher III
Lieutenant Junior Grade
United States Navy

Evanston, Illinois

June 1975

T163849

Thesis
[illegible]

DUDLEY KNOX LIBRARY
NAVAL POSTGRADUATE SCHOOL
MONTEREY, CALIFORNIA 93940

# Acknowledgements

I would like to thank Mr. E. N. Gigot of Allis Chalmers for providing the acceptance tests results for the modelled turbogenerator, the men of the Great Lakes Naval Training Station 1200 PSI Hot Plant for information on the entire turbogenerator system, and Mr. M. Young of NAVSHIPS Hyattsville for providing the design specifications for the turbine.

My sincere thanks to Dr. F. M. Brasch without whose help and suggestions this thesis would not have been possible.

And my graditude to my wife Jean for putting up with the endless hours of work spent on this thesis.

# ABSTRACT

This thesis reports on a study involving the simulation and control of a shipboard generating system (1000KW). The first part of the paper deals with the simulation of the existing system which includes a steam turbine, synchronous generator, voltage regulator and governor. Data on the system was obtained from the various manufacturers involved. Several simulations were made using different ways of modeling a synchronous machine that have been proposed in the literature, and their computational requirements compared. The models were comparable in the level of physical detail being represented and all were found to agree quite closely with test results.

The second part of the thesis reports on an attempt to control the system using a digital computer directly in the control loops. The simulation was repeated with the turbine and generator modeled as indicated above, while the voltage regulator and governor functions were implemented using relatively simple algorithms. For the degree of control needed in the shipboard environment these algorithms proved to be reasonably efficient and to give good results.

# TABLE OF CONTENTS

| | | |
|---|---|---|
| I | Introduction | 1 |
| II | The Development of the Model | 5 |
| III | The Development of the Digital Controller | 33 |
| IV | The Results of the Simulations | 43 |
| V | Conclusions | 58 |
| | Bibliography | 59 |
| A | Appendix | 61 |

# I INTRODUCTION

The modern steam powered ship is totally dependant on its ability to generate electric power. Steam powered may even be a misnomer since without electric power steam cannot be generated. Presently all that is steam powered is the turbogenerator, the main feed pumps, and the heating system. In the engineering plant the fuel oil pumps, the feed booster pumps, the condensate pumps, the fire and flushing pumps, and the cooling water pumps are electric powered. Even the automatic control system for the boiler requires electric power and cannot use steam power directly. Outside the engineering spaces everything is powered by electricity from the large electric motors for the steering system, for the gun and missile loaders and launchers, and for the anchor windless; to the complicated electronic communication, search and surveillance devices. Without a reliable source of electric power a modern ship is useless.

In order to reduce the operating costs of ships, automation is expanding into the shipboard environment. One area being investigated is the use of the digital computer to reduce the number of personnel required to operate the ship's engineering plant. The possibilities range from just using the computer for the collection and logging of data all the way to the

computer controlling the entire engineering plant. If such a computer were added to the engineering plant how could it best improve the generation of electricity aboard ship? One possibility is to replace the analogue controllers of the turbogenerators with a computer controller. This appears promising because of the special properties of a shipboard electrical system. On board ship the turbogenerators are located adjacent to each other. Normally the switchboard is located in an adjacent compartment with each generator connected to the bus line in this switchboard. The various shipboard loads are powered from this bus line. The generators are either totally connected at this point or the bus line is broken and each generator carries a seperate part of the load with no interconnection. In either case, mathematically the electric system would appear to be a single machine connected to a single load. In the shipboard system the main engines use about ninty-five percent of the steam produced. This means that the turbogenerators have such a large supply of steam that for analysis purposes it appears to be infinite. Thus, the boiler response does not enter into the turbogenerator system. Finally and most important, onboard ship the ratio of the change in electrical power required to the available electrical power is many times larger than is normally found in a large utility system. This results in larger fluctuations

in the turbogenerator parameters of frequency and terminal voltage. Thus the action of the controllers of these parameters are more easily seen and the extreme accuracy required in a large utility system is not expected to be met by the shipboard controllers.

In a shipboard environment there should be a simple efficient digital control scheme for the turbogenerator parameters of frequency and terminal voltage which would meet or exceed the response of the present controllers. Currently the frequency is controlled by a Watt flyball governor detecting speed changes and a hydraulic servo system translating these speed changes into changes in throttle position. This changes the power of the turbine and returns the speed to rated value. The current speed controller maintains speed within about four per cent of rated value under normal load conditions. It returns the speed to within two per cent of rated value in less than two seconds. The terminal voltage is controlled by a zener diode voltage sensing bridge, and a current transformer. The generator has a static excitor which uses the output of the current transformer as the input to a magnetic amplifier. The voltage sensing bridge controls the gain of the magnetic amplifier. The current transformer provides a vector sum of the terminal voltage and current, which aids the control function. Together the voltage controller maintains voltage within one per cent under normal conditions.

To find and test such a digital control scheme a model of the turbogenerator will be developed. A typical shipboard turbogenerator will be used for the basis of the model. The complete model will be tested against actual test results. A digital control scheme will be proposed. The digital controllers will replace the current controller in the model, and more simulations will be tested. The responses of the controllers will be compared.

During the development of the generator model the efficiency of the use of Parks' Transformation was questioned. To determine the order of magnitude of the savings and where these savings came from it was decided to try to simulate the model both with and without the use of Parks' Transformation.

# II THE DEVELOPMENT OF THE MODEL

## 2.I BACKGROUND

To insure authenticity of the control scheme the model is based on an actual shipboard type turbogenerator. The test results used to determine machine constants were provided by Allis Chalmers from the acceptance tests for the turbogenerator installed at Great Lakes Naval Station Training Plant. This is a mock up of a typical shipboard engineroom and is totally operational. The same model turbogenerator may be found in the Leahy Class Guided Missile Frigates (DLG-16).

The turbogenerator consists of a DeLaval 1442 BHP horizontal shaft condensing turbine. DeLaval speed reducing gears, an Allis Chalmers 1000 KW 450 Volt, 60 Cycle generator and static excitor, and Allis Chalmers auxiliary equipment.

Figure 1 shows the major parts of the shipboard environment. There are four boilers, two main engines, three turbogenerators, and much more major and minor auxiliary equipment, [1]. The boilers produce approximately 120,000 pounds of superheated steam (1200 PSI and 940°F) per hour. The majority of the steam goes directly to the main engines. A very small part is used for the few pieces of steam powered auxiliary equipment, primarily the main feed pumps, and a much smaller

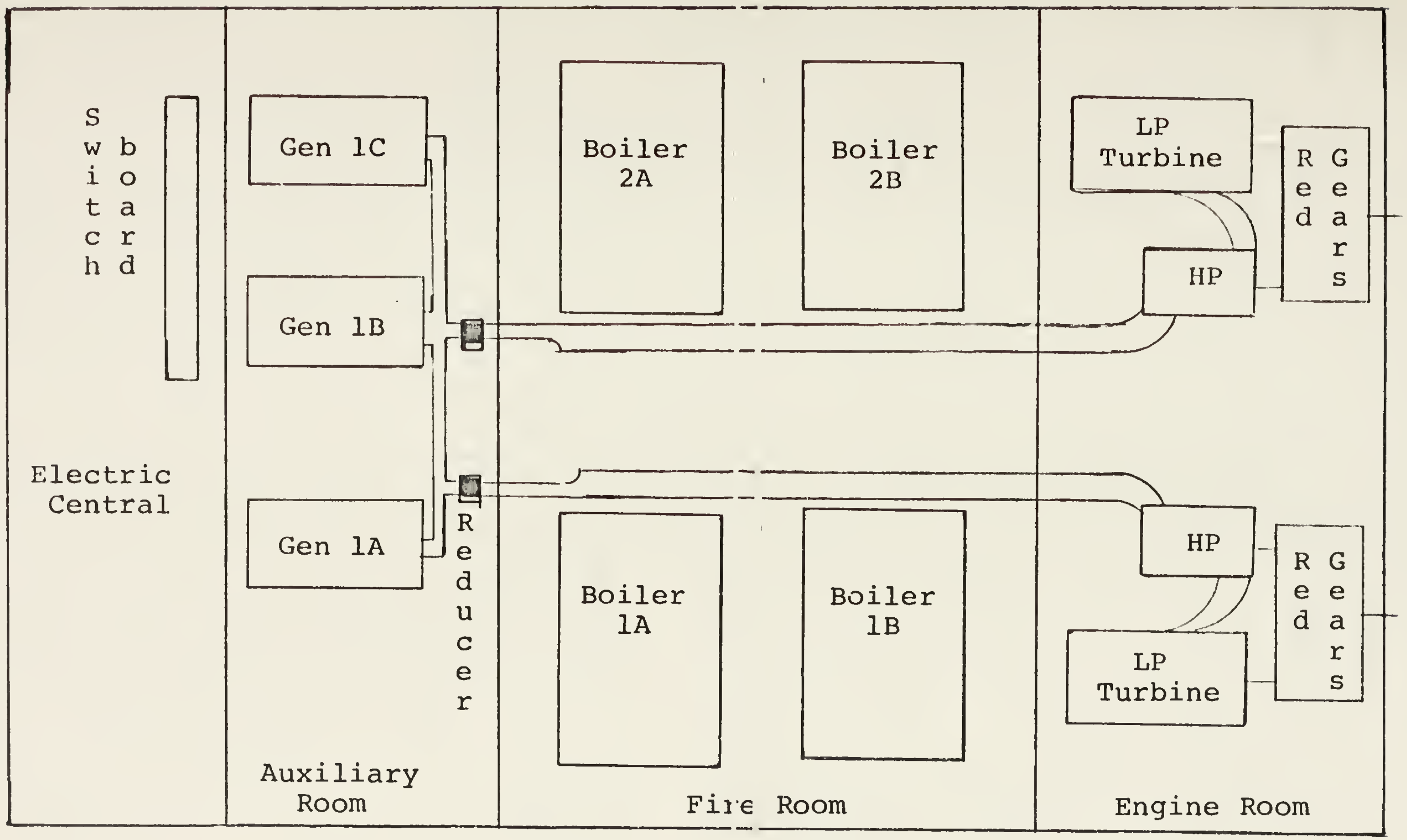
Switchboard
Electric Central
Gen 1C
Gen 1B
Gen 1A
Auxiliary Room
Reducer
Boiler 2A
Boiler 2B
Boiler 1A
Boiler 1B
Fire Room
LP Turbine
HP
Red Gears
HP
LP Turbine
Red Gears
Engine Room

Figure 1

quantity is reduced to 150 PSI for hotel services such as heating, cooking, and hot water. Of course there is approximately 9000 pounds of steam per hour that is used to generate electricity. The turbogenerators receive steam via a reducer, thus, being supplied at 440 PSI and 740°F. The electrical output of the generators goes directly to the main switchboard where all the generators are connected to the one bus line.

From this information two basic assumptions will be drawn. First since the turbogenerators use such a small portion of the available steam and the steam that they use is provided via a reducer, the turbogenerators appear to have an infinite supply of steam at constant temperature and pressure. Second since the turbogenerators are physically and electrically close they appear as a single machine supplying a single load.

Throughout the paper the quantities will be expressed in per unit notation unless otherwise specified. The bases for the per unit system are as follows:

| | |
|---|---|
| Volt Amperes | 1 p.u. = 1250 KVA |
| Volts | 1 p.u. = 260 Volts |
| Amperes | 1 p.u. = 1604 Amps |
| Rotor Volts | 1 p.u. = 54065 Volts |
| Rotor Amperes | 1 p.u. = 11.66 Amps |
| Frequency | 1 p.u. = 377 Radians per second |
| Steam Flow | 1 p.u. = 10,000 lbs per hour |
| Impedence | 1 p.u. = .1621 Ohms |

## 2.2 THE TURBINE

The DeLaval turbine of the turbogenerator is a 9 stage 10,009 RPM condensing turbine [2]. It receives steam at 440 PSI and 740$^{o}$F and exhausts to 4 inches of mercury absolute. (Condensors operate at pressures below atmospheric pressure and thus, to more accurately define the vapor point in the condensor, the pressure is measured in inches of mercury.) The turbine is capable of carrying its rated load continuously. The system is shown in figure 2.

Steam flow to the turbine is controlled by the throttle admitting steam to three nozzles progressively. In periods of low demand the steam is admitted only to the first nozzle. As the power required increases steam is also admitted to the second nozzle. Finally under periods of near full load conditions, steam is admitted to all three nozzles. All of the steam admitted to the first nozzle also passes through the second and third nozzles. The nozzles convert the potential energy of the steam to kinetic energy by accelerating the vapor molecules. Kinetic energy of the vapor molecules is transferred to the rotating energy of the turbine by striking the turbines blades. The first two stages (after the first nozzle) receive the steam at its highest temperature and pressure and convert the energy without allowing the steam to expand further. These stages are called impulse stages. They reverse the flow of vapor

Figure 2

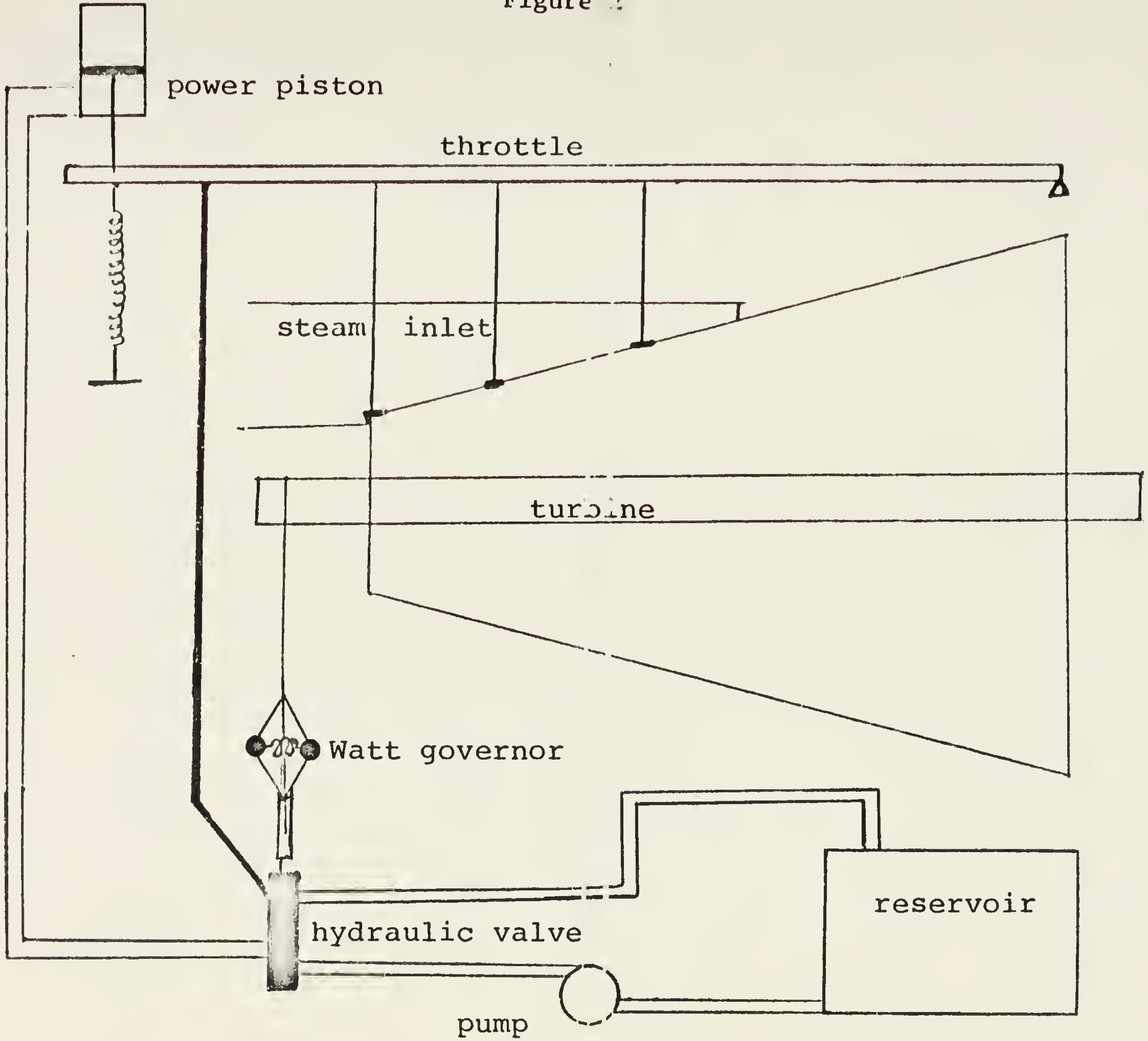
power piston
throttle
steam inlet
turbine
Watt governor
hydraulic valve
reservoir
pump

molecules without changing its velocity relative to the rotating blades. The remaining seven stages (three after the second nozzle and four after the third nozzle) are reaction stages. These blades also reverse the flow of steam to recieve its energy, but additionally they act as partial nozzles accelerating the vapor molecules as they pass. This is accomplished by the exhaust side of the blades having a larger opening than the inlet side. The resulting drop in pressure accelerates the steam.

The majority of the steam passes through the first nozzle and down the entire length of the turbine. There is a delay from the time the steam is admitted to the steam chest around the first nozzle until it actually passes through the nozzle. As the steam reaches the turbine blading it imparts more of its energy at each stage. The turbine power is measured to be linearly proportional to the steam flow. (See graph 1.) The turbine time constant is associated with the delay and transient time of the steam passing through the turbine. The turbine time constant, $T_{ch}$, controls the rate of change of the turbine power, TP, caused by the throttle position, VP, [3].

$$\dot{TP} = (VP - TP)/T_{ch} \qquad 2.2.1$$

By integrating this equation instantaneous turbine power may be found.

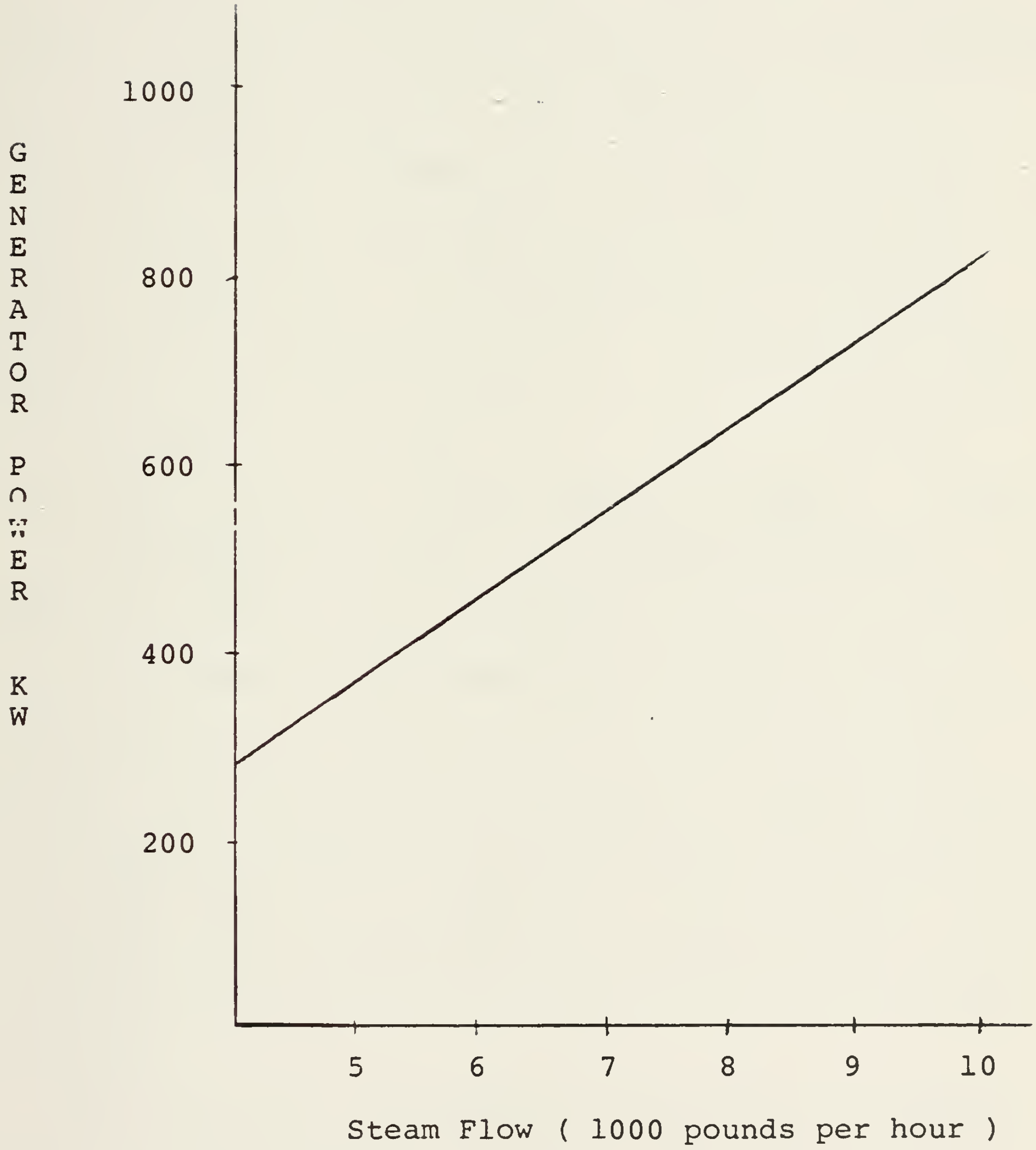
1000
800
600
400
200
GENERATOR POWER KW
5
6
7
8
9
10
Steam Flow ( 1000 pounds per hour )

Graph 1

## 2.3 THE MECHANICAL SYSTEM

From the current turbine power a value for the speed of the turbine may be calculated. Since power must be conserved the difference of the turbine power produced minus the electrical power and the lost power must appear as a change in angular momentum. The only method of changing the angular momentum of the turbogenerator is by accelerating it. The acceleration of the turbogenerator, $\dot{\omega}$, is equal to the difference of the power produced and the power required divided by the inertia constant, 2H. This acceleration is also the acceleration of the power angle, $\ddot{\delta}$. Since Torque times speed is equal to the power:

$$\ddot{\delta} = \dot{\omega} = ( TP - [ T_{ele} + T_{loss} ]^{*} \omega)/_{2H} \qquad 2.3.1$$

The inertia constant, H, is computed from the moment of inertia of the turbogenerator and its rated speed. By knowing the dimensions and weight of the rotating parts the moment of inertia can be computed. However, the difference in the speed of rotation between the turbine and generator must be taken into consideration. The larger radius of the generator and gear dominate the inertia constant despite the larger speed of the turbine and pinion.

The term $T_{loss}$ in equation 2.3.1 is an approximation of all the mechanical losses. The largest part is due to the speed reducing gear. Friction losses in the

bearings are also included, as well as windage losses in the generator. The sum of the losses was assumed to be equal to the total power required to maintain rated speed with no field excitation. This value is $T_{loss}$ = .1 p.u. or 1000 lbs of steam per hour, [2].

## 2.4 THE SPEED CONTROLLER

The throttle position is controlled by the governor. The Watt governor measures the turbine shaft speed by means of a flyball arrangement. Attached to the shaft of the governor are two opposing balls on a pivoted linkage. The balls may move easily in a radial direction and are forced to rotate with the shaft. The two balls are connected by a spring. The spring exerts the force required to make the balls travel in a circular path about the shaft. As the shaft's speed increases more force is required to continue to accelerate the balls to their circular path, and the spring stretches increasing the force it exerts, and enlarging the radius of the circular path of the balls. Another linkage connected to the balls detects the increase in the radius of the circular path of the balls and uses this movement to displace a valve. The movement of the valve causes a pressure difference between the hydraulic pressure in the power piston tending to open the throttle, and the spring trying to close the throttle. The power piston moves to equalize the forces and in so moving returns the

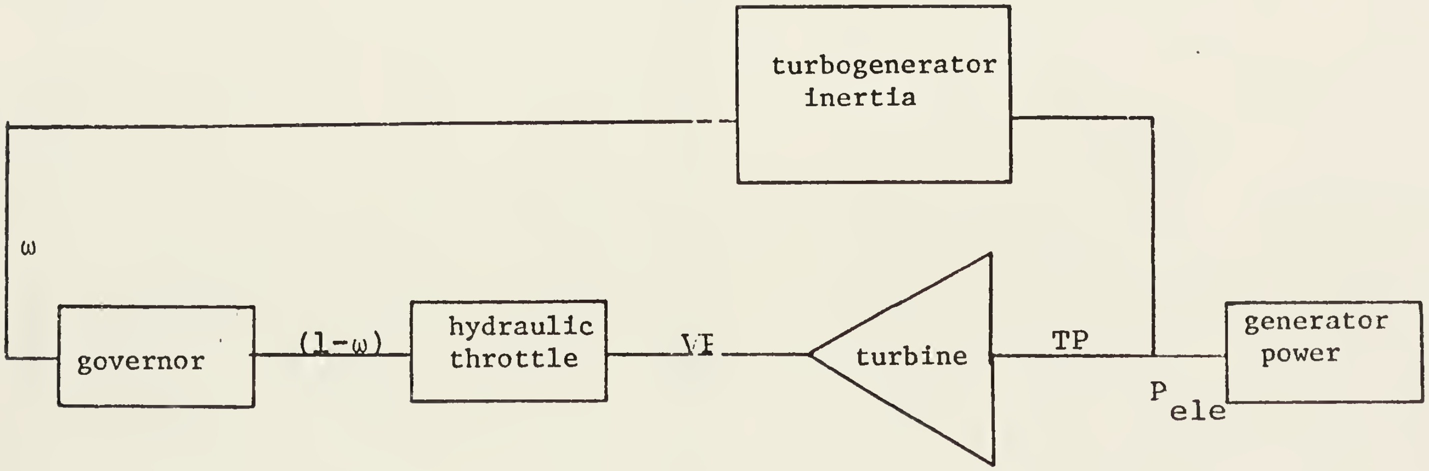
turbogenerator inertia
ω
governor
(1-ω)
hydraulic throttle
VF
turbine
TP
$P_{ele}$
generator power

Figure 3
(From Reference 3)

valve to its neutral position. The rate of change of the throttle depends on an error signal from the governor, $1-\omega$, amplified by the hydraulic system and combined with the old throttle position, DVP, minus the current throttle position, VP, divided by the time constant of the hydraulic servo system. The delayed throttle position may be found by integrating the throttle position minus the delayed throttle position divided by the time constant, [3].

$$\dot{VP} = ( DVP - VP + [ 1-\omega ]*35 ) /_{75.4} \qquad 2.4.1$$

$$\dot{DVP} = ( VP - DVP )/_{302} \qquad 2.4.2$$

The governor maintains speed within 4% of rated value and returns to a steady state speed of within 2% of rated value in less than two seconds under normal load fluctuations.

## 2.5 THE GENERATOR

The Allis Chalmers generator is a 1000 KW, 0.8 Power Factor, 450 Volt 3 Phase, 60 cycle totally enclosed synchronous A.C. generator, [2] and [7]. It is a salient pole type machine operating at 1200 RPM. The rotor receives direct current through four brushes on two rings from a static excitor. The rotor has complete damper windings in the pole faces. The stator has 90 coils, connected in groups of five coils. There are six of these groups per phase with the phases connected in a Y circuit (see figure 4). The air gap is approximately

0.185 inches. Both the rotor and stator are punched from electrical sheet steel with each sheet insulated. The generator is air cooled.

Three basic assumptions are made in modeling the electric and magnetic circuits. The first assumption is that each phase is identical and that each coil in each phase is identical so that the model will be described as a two pole machine (see figure 5). Even though the amortissieurs are continuous about the rotor, mathematically they will be viewed as being symmetric about the direct and quadrature axes so that no mutual components exist between the direct and quadrature axis amortissieur. The final assumption, in steady state, all flux distributions vary as sinusoids in space, [4] and [5].

According to Faraday's Law, the voltage induced in a circuit is equal to the rate of change of flux linkage. Assuming the resistance of the three phases are equal, the phase voltages, $e_a$ $e_b$ $e_c$, are equal to the rate of change of flux, $d\Psi/dt$, minus the phase current, $i_a$ $i_b$ $i_c$, times the phase resistance, r.

$$\begin{aligned} e_a &= d\Psi_a/dt - ri_a \\ e_b &= d\Psi_b/dt - ri_b \qquad 2.5.1 \\ e_c &= d\Psi_c/dt - ri_c \end{aligned}$$

The flux linkages in the phases result from the currents flowing in all the coils of the generator. The self and

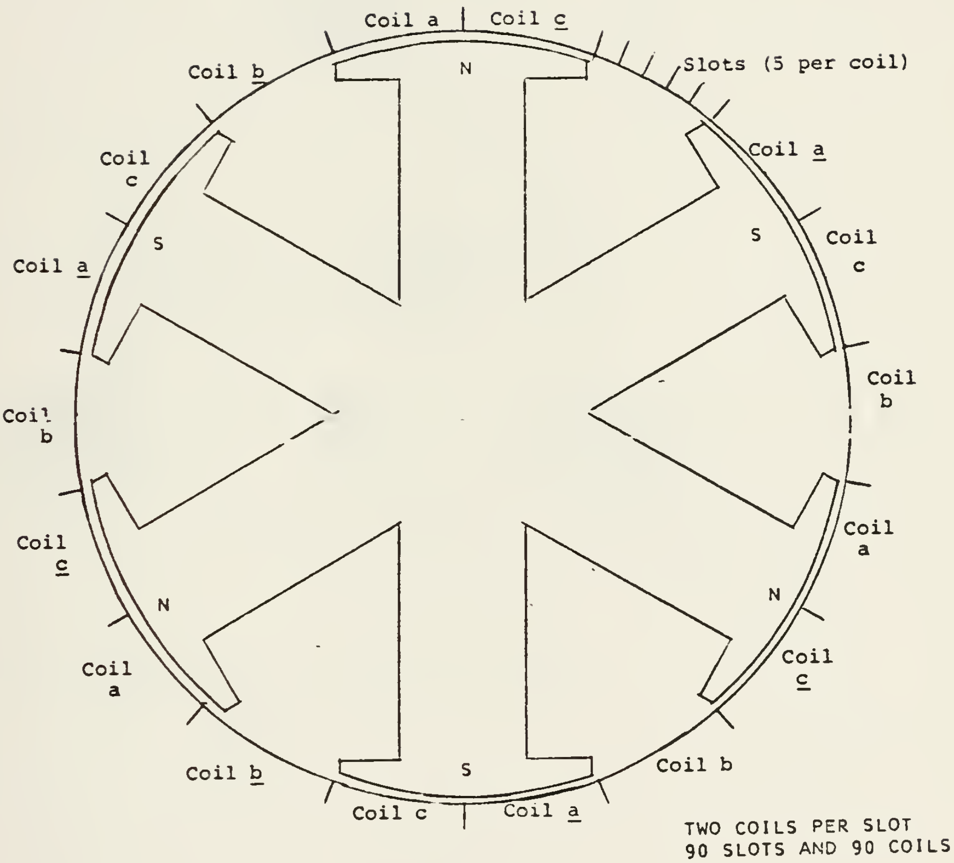
Coil a
Coil c
Slots (5 per coil)
Coil b
N
Coil a
Coil c
S
S
Coil c
Coil a
Coil b
Coil b
Coil a
Coil c
N
N
Coil c
Coil a
Coil b
S
Coil b
Coil c
Coil a
TWO COILS PER SLOT
90 SLOTS AND 90 COILS

FIGURE 4

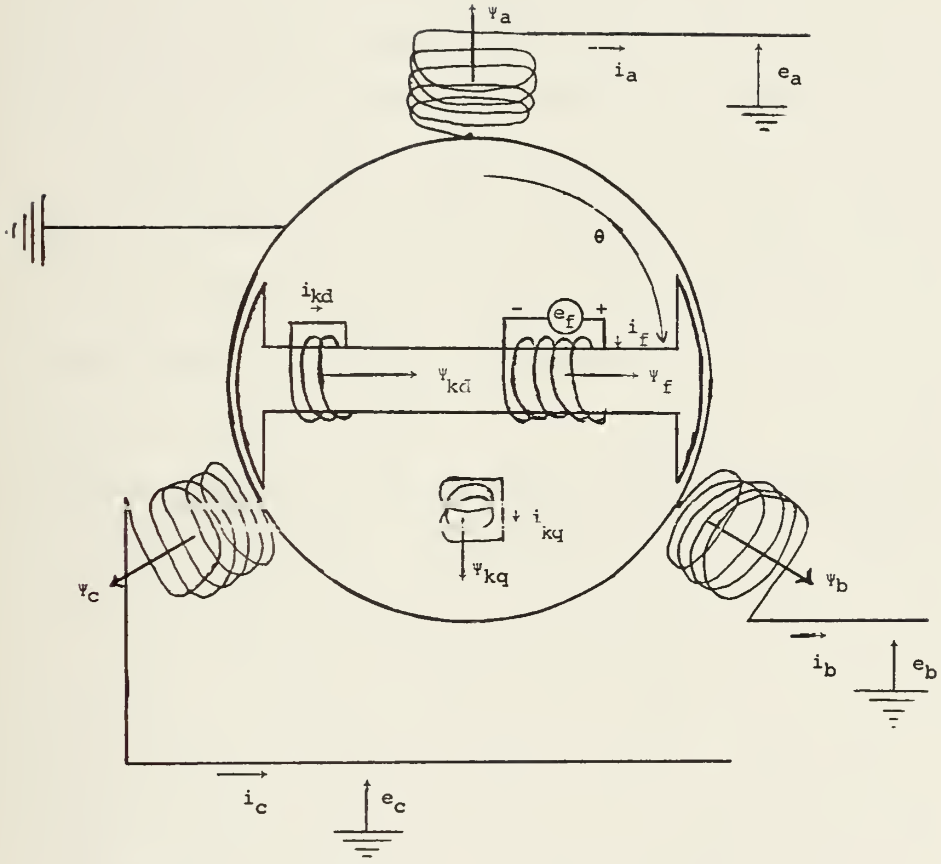
$\Psi_a$
$i_a$
$e_a$
$\theta$
$i_{kd}$
$e_f$
$-$
$+$
$i_f$
$\Psi_{kd}$
$\Psi_f$
$i_{kq}$
$\Psi_{kq}$
$\Psi_c$
$\Psi_b$
$i_b$
$e_b$
$i_c$
$e_c$

FIGURE 5

mutual inductances of these coils may vary with the rotor angle, $\theta$. Since the three phases are assumed to be identical except for being 120 degrees apart, only the a phase will be described. By adding 120 degrees to the rotor angle at every occurence the inductances of the b phase will be found. Likewise by subtracting 120 degrees from the rotor angle the inductances of the c phase will be found. The self inductances of the a phase is expressed by an even Fourier series of the rotor angle. The first term, a constant $L_{aa0}$, results from the actual inductances of the a phase coil by itself. The next term, $L_{aa2}\cos 2\theta$, is proportional to the cosine of twice the rotor angle. This term is solely due to the salience of the rotor alternately decreasing and increasing the reluctance to the stator coils. Since the sum of the frequency components, other than the component at 60 Hertz, of the terminal voltage and current is measured to be less than 2% of rated value, only these first two terms of the Fourier series will be considered. If the frequency components of the generator output were to be studied then the Fourier series would have to be extended to encompass more terms [6]. The self inductance of the a phase is $-L_{aa0}-L_{aa2}\cos 2\theta$. It is negative so that current out of the generator will represent positive power. (See figure 5 for all sign convention.) The mutual inductances between the phases is also expressed

as a Fourier series. The constant term, $L_{ab0}$, is solely due to the phase coils alone. The same second term appears in the series. However the reluctance is now at a minimum when the pole face is half way between the two phases, a to b $L_{ab0} + L_{aa2}\cos 2\theta+60$; a to c $L_{ab0} + L_{aa2}\cos 2\theta-60$. The mutual inductances between the rotor and phase a depend completely on the rotor angle. Since the field coil and mathematical direct axis amortissieur act along the same axis they appear mathematically similar. The mutual inductance from the field, $L_{af}\cos\theta$, and from the direct axis amortissieur, $L_{akd}\cos\theta$, are at a maximum when the north pole, positive flux, of the rotor is inline with the a phase. The quadrature axis amortissieur behaves similarly, except that it is mathematically 90 degrees ahead of the direct axis. The mutual inductance of the quadrature axis amortissieur, $L_{akq}\sin\theta$, is a maximum 90 degrees before the a phase is inline with the rotor. Again the inductances of phases b and c are 120 degrees ahead and behind the a phase. Since the stator is totally symmetric (disregarding slots) the self and mutual inductances of the rotor coils are constants, $L_f$ for the field coil; $L_{kd}$ for the direct axis amortissieur; and $L_{kq}$ for the quadrature axis amortissieur. There is mutual inductance between the field and direct axis, $L_{fkd}$, but since the quadrature axis is 90 degrees apart there is no flux linkage between them. From this

information an inductance matrix, $\underline{L}$, may be formed. The flux linkage, $\Psi$, is then equal to the inductance times the current, or in matrix form:

$$\underline{\Psi} = \underline{L} * \underline{i} \qquad 2.5.2$$

See figure 6 for $\underline{L}$.

The phase voltages, $e_a$ $e_b$ $e_c$, have been discussed once in equation 2.5.1, however they may also be found in relation to the generator's load. That is the voltage is equal to the current generated, $i_a$ $i_b$ $i_c$, times the load, $R_{load} + L_{load}$.

$$\begin{aligned} e_a &= R_{load} * i_a + L_{load} * di_a/dt \\ e_b &= R_{load} * i_b + L_{load} * di_b/dt \qquad 2.5.3 \\ e_c &= R_{load} * i_c + L_{load} * di_c/dt \end{aligned}$$

The field voltage is derived from the exciter's output and will be discussed later. The amortissieur coils are shorted.

The generator may be modelled by the following matrix equations [4], [5], and [8]:

$$d\underline{\Psi}/dt = \underline{e} - r*\underline{i} \qquad 2.5.1$$

$$\underline{i} = \underline{L}^{-1} * \underline{\Psi} \qquad 2.5.2$$

$$\underline{e} = \underline{R}_{load} * \underline{i} + \underline{L}_{load} * d\underline{i}/dt \qquad 2.5.3$$

$$\underline{\Psi} = (\Psi_a \ \Psi_b \ \Psi_c \ \Psi_f \ \Psi_{kd} \ \Psi_{kq}) \qquad 2.5.4$$

$$\underline{e} = (e_a \ e_b \ e_c \ e_f \ 0 \quad 0 \ ) \qquad 2.5.5$$

$$\underline{i} = (i_a \ i_b \ i_c \ i_f \ i_{kd} \ i_{kq}) \qquad 2.5.6$$

$\underline{L}$ is as in figure 6.

$$\underline{r} = \text{diagonal} \ ( -r_a \ -r_a \ -r_a \ r_f \ r_{kd} \ r_{kq}) \qquad 2.5.7$$

$$\begin{bmatrix} \Psi_a \\ \Psi_b \\ \Psi_c \\ \Psi_f \\ \Psi_{kd} \\ \Psi_{kq} \end{bmatrix} = \begin{bmatrix} -L_{aa0}-L_{aa2}\cos(2\theta) & L_{ab0}+L_{aa2}\cos(2\theta+60) & L_{ab0}+L_{aa2}\cos(2\theta+300) & L_{af}\cos(\theta) & L_{akd}\cos(\theta) & -L_{akq}\sin(\theta) \\ L_{ab0}+L_{aa2}\cos(2\theta+60) & -L_{aa0}-L_{aa2}\cos(2\theta-240) & L_{ab0}+L_{aa2}\cos(2\theta-180) & L_{af}\cos(\theta-120) & L_{akd}\cos(\theta-120) & -L_{akq}\sin(\theta-120) \\ L_{ab0}+L_{aa2}\cos(2\theta+300) & L_{ab0}+L_{aa2}\cos(2\theta-180) & -L_{aa0}-L_{aa2}\cos(2\theta+240) & L_{af}\cos(\theta+120) & L_{akd}\cos(\theta+120) & -L_{akq}\sin(\theta+120) \\ -L_{af}\cos(\theta) & -L_{af}\cos(\theta-120) & -L_{af}\cos(\theta+120) & L_f & L_{fkd} & 0 \\ -L_{akd}\cos(\theta) & -L_{akd}\cos(\theta-120) & -L_{akd}\cos(\theta+120) & L_{fkd} & L_{kd} & 0 \\ L_{akq}\sin(\theta) & L_{akq}\sin(\theta-120) & L_{akq}\sin(\theta+120) & 0 & 0 & L_{kq} \end{bmatrix} * \begin{bmatrix} i_a \\ i_b \\ i_c \\ i_f \\ i_{kd} \\ i_{kq} \end{bmatrix}$$

Figure 6
Equation 2.5.2

$$d\underline{i}/dt = (\underline{L} + L_{load})^{-1} * (\underline{e} + \underline{r}*\underline{i} - d\underline{L}/dt * \underline{i}) \quad 2.5.8$$

This three phase model may be simplified by the use of a coordinate transformation. The new equations, known as Parks' equations, will form a model identical to equations 2.5.1 to 2.5.8. The coordinate transformation will remove the dependance on rotor angle from the inductance matrix $\underline{L}$. This model will be called the dq0 model. The transformation is as follows:

$$T = \begin{bmatrix} {}^2/_3\cos\theta_a & {}^2/_3\cos\theta_b & {}^2/_3\cos\theta_c & 0 & 0 & 0 \\ -{}^2/_3\sin\theta_a & -{}^2/_3\sin\theta_b & -{}^2/_3\sin\theta_c & 0 & 0 & 0 \\ {}^1/_3 & {}^1/_3 & {}^1/_3 & 0 & 0 & 0 \\ 0 & 0 & 0 & {}^2/_3 & 0 & 0 \\ 0 & 0 & 0 & 0 & {}^2/_3 & 0 \\ 0 & 0 & 0 & 0 & 0 & {}^2/_3 \end{bmatrix}$$

$\theta_a = \theta$

$\theta_b = \theta + 120$

$\theta_c = \theta - 120$

$$T^{-1} = \begin{bmatrix} \cos\theta_a & -\sin\theta_a & 1 & 0 & 0 & 0 \\ \cos\theta_b & -\sin\theta_b & 1 & 0 & 0 & 0 \\ \cos\theta_c & -\sin\theta_c & 1 & 0 & 0 & 0 \\ 0 & 0 & 0 & {}^3/_2 & 0 & 0 \\ 0 & 0 & 0 & 0 & {}^3/_2 & 0 \\ 0 & 0 & 0 & 0 & 0 & {}^3/_2 \end{bmatrix}$$

The current, voltage, and flux linkage matrices for the dq0 model are found by:

$$\underline{i}_{dq0} = T * \underline{i}_{3\phi} \qquad 2.5.9$$

$$\underline{e}_{dq0} = T * \underline{e}_{3\phi} \qquad 2.5.10$$

$$\underline{\Psi}_{dq0} = T * \underline{\Psi}_{3\phi} \qquad 2.5.11$$

The inductance matrix for the dq0 model is found by:

$$\underline{\Psi}_{3\phi} = \underline{L}_{3\phi} * \underline{i}_{3\phi}$$

$$T^{-1}\ \underline{\Psi}_{dq0} = L_{3\phi} * T^{-1}\ \underline{i}_{dq0}$$

$$\underline{\Psi}_{dq0} = T * L_{3\phi} * T^{-1}\ \underline{i}_{dq0}$$

$$L_{dq0} = T * L_{3\phi} * T^{-1} \qquad 2.5.12$$

$$L_{dq0} = \begin{bmatrix} -L_d & 0 & 0 & L_{df} & L_{dkd} & 0 \\ 0 & -L_q & 0 & 0 & 0 & L_{qkq} \\ 0 & 0 & -L_0 & 0 & 0 & 0 \\ -L_{df} & 0 & 0 & L_f & L_{fkd} & 0 \\ -L_{dkd} & 0 & 0 & L_{fkd} & L_{kd} & 0 \\ 0 & -L_{qkq} & 0 & 0 & 0 & L_{kq} \end{bmatrix} \qquad 2.5.13$$

$$L_d = L_{aa0} + L_{ab0} + {}^3/_2 L_{aa2}$$

$$L_q = L_{aa0} + L_{ab0} - {}^3/_2 L_{aa2} \qquad 2.5.14$$

$$L_0 = L_{aa0} - 2*L_{ab0}$$

All other quanities are 3/2 their three phase values. This model is advantageous because it is time invariant however it is still nonlinear because of the cross terms of frequency and flux.

$$d\Psi_d/dt = e_d - r * i_d + \omega * \Psi_q$$
$$d\Psi_q/dt = e_q - r * i_q - \omega * \Psi_d \qquad 2.5.15$$
$$d\Psi_0/dt = e_0 - r * i_0$$

The torque of the generator may be derived from the rate of change of air gap power [4] or for the three phase model

$$T_{ele} = {}^2/_3\sqrt{3}[\Psi_a(i_c-i_b)+\Psi_b(i_a-i_c)+\Psi_c(i_b-i_a)] \qquad 2.5.16$$

For the dq0 model

$$T_{ele} = \Psi_d * i_q - \Psi_q * i_d \qquad 2.5.17$$

## 2.6 THE VOLTAGE CONTROLLER

The excitor and voltage regulator are combined into one unit in this system. In all but the initial starting of the turbogenerator, the excitation is derived from the rectified terminal voltage and current. The initial field flashing voltage is obtained from a permanent magnet alternator attached to the generator shaft. At times other than starting it is used as a tachometer to the main switchboard. It is capable of supplying enough excitation to produce one half the rated terminal voltage at no load and is disconnected electrically from the system at all other times.

The normal excitation is derived from a set of three magnetic amplifiers, one for each phase. The magnetic amplifiers have three inputs, a saturation input, a signal input, and a control input. A current transformer across one phase of the generator provides two of these. The current transformer has windings both parallel to and in series with the terminal. The potential windings provide power when the generator is in a no load condition, whereas, the current coil provide power if a short circuit develops. Under normal conditions the current transformer produces an output proportional to the vector sum of the terminal voltage and the terminal current. The transformer's output is rectified to provide the saturation input to the magnetic amplifier. The output is also the signal input to the magnetic amplifier. The control signal is derived by an error detecting circuit to be described later. The output of the magnetic amplifier goes to a three phase rectifier with the other two magnetic amplifiers. This rectified output is the source of excitation voltage. There is a free wheeling diode across the field terminals to provide a path for the field current during short periods of low voltage from the magnetic amplifiers.

The actual control of the magnetic amplifiers is

derived from a pair of potential transformers which form an open bridge in the generator's terminal lines. The output of the transformers is input to a voltage sensing bridge of two zener diodes and two resistors. The voltage error signal is amplified by a magnetic amplifier. A damping signal, derived from a RC differentating network in the excitor terminals, is subtracted from the error signal. The resulting signal is smoothed and used to alter the gain of the three main magnetic amplifiers.

Two separate actions occur when the load of the generator is altered. First the input signal of the main field magnetic amplifier is modified. This is the vector sum of terminal voltage and current. As the load is increased the terminal current increases, increasing the vector sum. If the terminal voltage were to remain at rated value this change alone would maintain the necessary excitation. But the terminal voltage does not stay constant. As it changes the error detector circuit alters the gain of the magnetic amplifier to try to return the terminal voltage to rated value. These two signals working together improve the response of the terminal voltage beyond the response either signal alone is capable of producing.

The model for this static excitor and voltage regulator is based on a IEEE Standard type three system

from [9]. The output of the current transformer, TER, is the sum of the magnitude of terminal voltage, VT, plus the magnitude of the terminal current, TI, times the power angle. Since the values are rectified the actual phase angles are not important. The error detector circuit produces a signal, ERR, which is the rated per unit terminal voltage minus the normalized terminal voltage. The stabilization signal, STAB, is found from the derivative of the field voltage, $\dot{e}_f$, integrated with the old stabilization signal. The change of the magnetic amplifier gain is integrated from the old gain, SIG, and the error signal and the stabilization signal. Thus

$$\begin{aligned} TER &= VT + TI * PF \\ ERR &= 1 - VT \\ \dot{STAB} &= -{}^{1}/_{T_f} * STAB + {}^{K_f}/_{T_f} * \dot{e}_f \qquad 2.6.1 \\ \dot{SIG} &= -{}^{1}/_{T_a} * SIG + {}^{K_a}/_{T_a} * (ERR-STAB) \\ e_f &= ( 1 + SIG ) * TER \end{aligned}$$

(See figure 7 .)

Ka and Ta are parameters of the main field magnetic amplifiers. Kf and Tf are parameters of the error circuit magnetic amplifier.

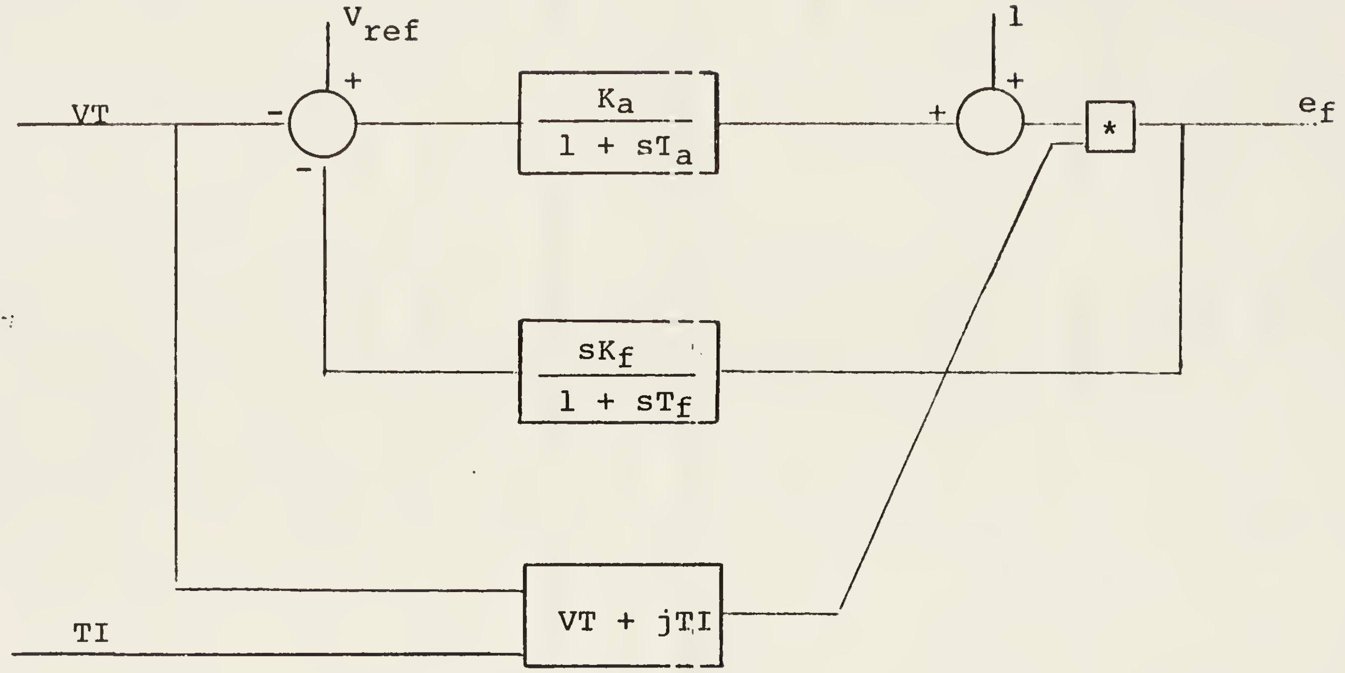

$V_{ref}$
1
+
+
VT
-
-
+
$\frac{K_a}{1 + sT_a}$
*
$e_f$
$\frac{sK_f}{1 + sT_f}$
TI
VT + jTI

Figure 7

## 2.7 SIMULATION OF THE MODEL

The models were assembled by parts to form a complete model of the turbogenerator. The model was simulated on a digital computer by a fourth order Runga Kutta type algorithm. It was not a true Runga Kutta scheme, since the solution was found in two steps. First the generator model was solved for one step under constant excitation and rotation. The voltage regulator, the speed controller, and the mechanical system were stepped forward one step under constant generator output. Each step provided the input for the next step. The method provided satisfactory simulation because of the large differences in the time constants of the two parts of the system. In this manner the two generator models could be easily interchanged as well as the new controllers.

The three phase generator model required the smallest step size and the largest computing time. The smaller step size resulted from the currents and voltages in this model remaining sinusiodal. The longer computing time resulted from the inversion of the induction matrix at each step.

The advantages of the three phase model were that the outputs are actual machine quantities. The model would also accept any conceivable load conditions. The model is capable of being more accurate in its simulation since exact coil inductances may be included. This

allows the model to accept possible differences in the three phases.

The dq0 model can be simulated in much the same manner as the three phase. However, the dq0 is time invariant, thus the inductance matrix need only be inverted once. By proper matrix manipulation the required computations for this model may be reduced. Since the transformation removes the frequency component associated with the rotor angle ( the highest frequency oscillation and the only undamped oscillation) a varible step size may be used to increase the step size as the oscillations disappear. All of this results in a model that the computer may execute much faster than the three phase model.

The dq0 model is restricted in simulating unbalanced loads. To accomplish this the output must be converted to phase quantities, the load values computed and then transformed back to dq0 values. This still requires less time to accomplish than the three phase model requires to invert the inductance matrix. The dq0 model may not include any differences between the three phases.

In future studies saturation should be included in both models. In the three phase model the inductances of each coil would be varied by the current flowing in them to represent the saturation. This would not significantly affect the model. However, in the dq0

model if the inductances had to be altered for saturation the matrix would have to be reinverted at each change in saturation. This could significantly reduce the speed of execution of the dq0 model.

## 2.8 TESTING THE MODEL

Both models were tested under the following conditions:

No load to full load

No load to short circuit

Full Load to partial load

The models were found to compare satisfactorily in all respects with each other as well as with the provided acceptance tests for the turbogenerator. The actual simulation run results may be found in Section 4.

# III THE DEVELOPMENT OF THE DIGITAL CONTROLLERS

In the introduction several proprieties of the shipboard environment were introduced which would enchance a simple control scheme. The elimination of the boiler from the model has been discussed. This also allows the speed controller to operate without determining the steam power available. It appears to be a constant infinite supply. The voltage regulator will not have to be able to dampen oscillations caused by a multi-machine environment since there appears to only be one machine and one load. Finally both controllers have leeway in the control. The output does not have to be exact at all times.

This thesis will not attempt to build these controllers. Only the simple control scheme will be proposed. Developing the hardware required to actually build the controller will be left to a future study.

## 3.1 THE DIGITAL VOLTAGE REGULATOR

The first and most obvious method of finding a digital control scheme is to implement the present controller in digital form. The present controller consists of an error detecting circuit. The main field magnetic amplifier provides the power source for excitation. The proposed digital controller will only control the output of the magnetic amplifier. The current controller model is:

$$\dot{STAB} = -{}^{1}/_{T_f} * STAB + {}^{K_f}/_{T_f} * \dot{e}_f \qquad 2.6.3$$

$$\dot{SIG} = -{}^{1}/_{T_a} * SIG + {}^{K_a}/_{T_a} * (ERR-STAB) \qquad 2.6.4$$

In digital, z transform, form with a sampling period of T the following transfer equations would result:

$$\frac{STAB(z)}{e_f(z)} = \frac{K_f/T_f \; z}{z - e^{-T/T_f}} \qquad 3.1.1$$

$$\frac{SIG(z)}{(ERR-STAB)(z)} = \frac{K_a/T_a \; z}{z - e^{-T/T_a}} \qquad 3.1.2$$

The difference equations provide a better feel for what this proposed AVR would require:

$$STAB[(k+1)T] = {}^{K_f}/_{T_f} * e_f[(k+1)T] + e^{-T/T_f} * STAB[kT]$$

$$SIG[(k+1)T] = {}^{K_a}/_{T_a} * (ERR-STAB)[(k+1)T] + e^{-T/T_a} \; SIG[kT]$$

To implement this proposed digital information on AVR the terminal voltage, or error signal, and on the field voltage, or its derivitive, would have to be provided digitally. The former signal in each case would require processing to arrive at the needed signal. The voltage regulator could be greatly improved by the use of some functions easily performed digitally but which in the analogue world would be extremely difficult. A very simple generator model would be, [15]

$$VT = ki_f - jIX_s \qquad 3.1.3$$

Where VT is terminal voltage, I is terminal current, $X_s$ is synchronous reactance and k is a constant. This model

shows that the required excitation current is related to the real current. Thus if the real current could be calculated the exact excitation current would be known. The real current depends on the exact load and the rotor angle. It is difficult to compute.

An easier method of approximating the required excitation comes from equation 3.1.3. By measuring the instantaneous terminal voltage and field current an approximation of the field current required to return to the rated terminal voltage conditions would be ${}^{i}f/_{VT}$. This assumes that everything else remains constant. To see this the model must be examined. By normalizing the rated terminal voltage to one then forming a proportionality:

$$\frac{VT}{1} = \frac{-k*i_f - j\ I*X_s}{-k*i_f' - j\ I'*X_s} \qquad 3.1.4$$

(The prime quantities are the desired values.)

But under constant rotor angle: $I' = {}^{I}/_{VT}$

Thus the desired relationship: $i_f' = {}^{i}f/_{VT}$

Although this is a good approximation, it is not exact. The major fault is that neither the rotor angle, nor the load, remains constant. The real current is therefore not always proportional to the terminal voltage. However, since the field current cannot be changed instantaneously, several new approximations can

be made updating the required field current before the generator can completely readjust to the new load.

To insure this procedure works correctly it must be shown that it quickly produces the correct estimate of the required field current, and that it will maintain this correct estimate. The estimate can be viewed as being proportional to the instantaneous power demanded of the generator. Under this instantaneous power requirement the excitation current must be increased to increase the terminal voltage. In some possible load changes (such as application of a large resistive load from noload conditions) the instantaneous power requirement is not even in the same direction from the previous power required as the steady state power requirement of the new load. (Under application of full resistive load the intial terminal voltage rises indicating less power is required although the steady state power requirement is larger than the present requirement.) The estimate of the required excitation must be updated regularly. At the next estimate the instantaneous power requirement and rotor angle will be closer to the steady state values, and will produce a better estimate to the required steady state excitation. Requiring a new estimate to be calculated before the field current can significantly change will insure that the power will not be changed in the wrong direction.

The procedure might be better explained graphically in figure 8. Here the generator is at steady state under the original power requirement. The load is then altered. Since the field current cannot change instantaneously the terminal voltage drops toward the new load line. The AVR assumes the load has not changed and raises the excitation voltage proportional to the terminal voltage, to return the terminal voltage under the original load to its rated value. At the next approximation the field current is increased and the terminal voltage is still below rated value. Notice that the approximations are at a high enough rate to prevent the field current from significantly changing between approximations. Even though the field current has been increased the terminal voltage is not at its rated value. The AVR estimates the new power requirement and computes a new estimate of the required field current. The process converges rapidly to the correct terminal voltage, and the AVR no longer attempts to change the field current. The AVR thus always produces a better estimate of the required field current and steadies out at rated value.

Although this proposed AVR works, it is slow to respond because of the large time constant of the field circuit. To improve the rate of change of field current the excitation voltage applied to the field must be larger than required. An easy method to overcompensate the field voltage is to use $i_f/(V_T)^2$ as the voltage signal.

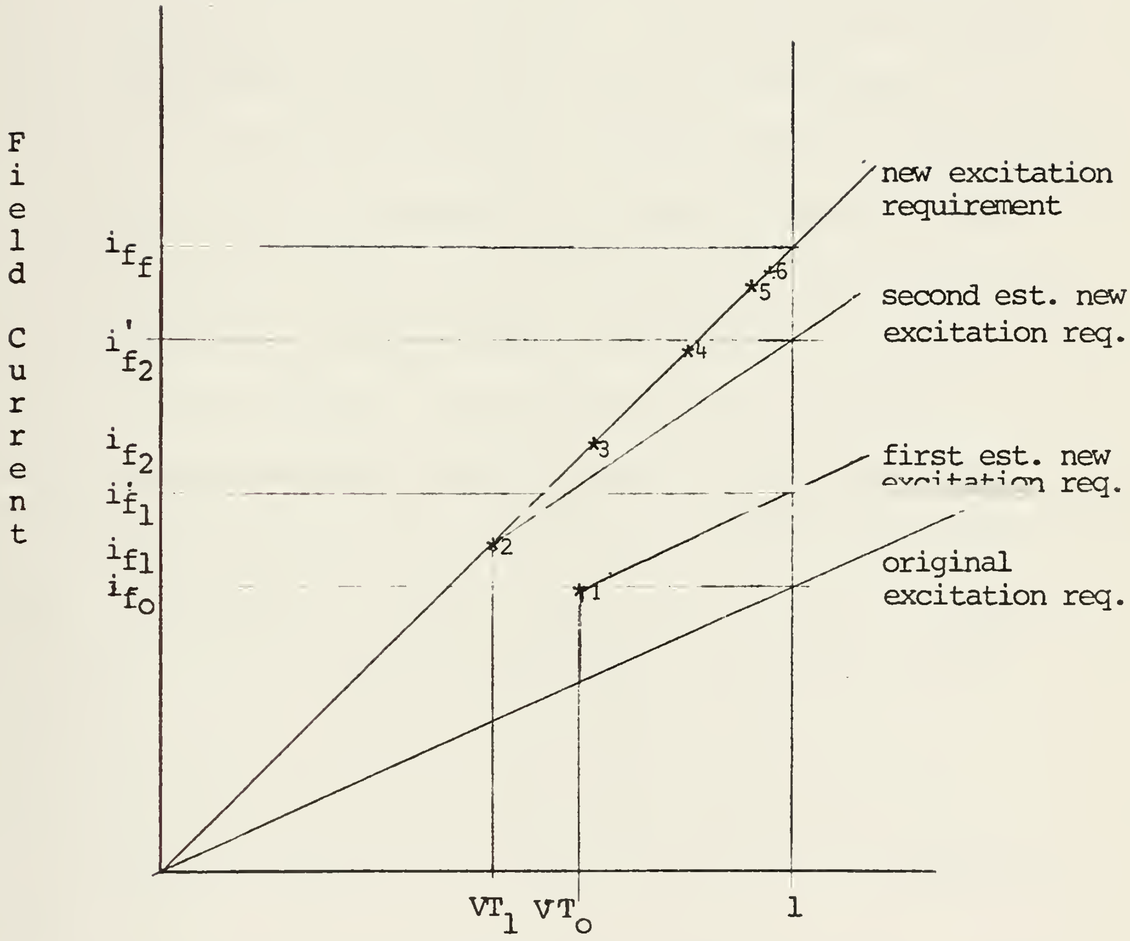

( The * represent new approximations are being made by the AVR. )

Figure 8

Then the voltage will be exact when at unity and will be overcompensating at all other times. The field current will therefore respond to change faster than if just the required voltage were applied. To improve even further, if the terminal voltage varies more than a preset amount from rated value the AVR would push the excitor to its limits. Together these changes make the proposed digital AVR respond much faster, but the cost is that the terminal voltage tends to oscillate. To prevent this the AVR must calculate a new estimate of the required field current before the field current can significantly change under the maximum rate of change of the excitor. The samples must be often enough to prevent the terminal voltage from changing more than this preset amount before another sample is taken. The excitor voltage can then be set to a better estimate of the required excitation before the field current can pass through its required level. A sampling period of once every three radians, twice a cycle, appears under most conditions to be an adaquate rate.

To implement the proposed digital automatic voltage regulator, the following tests of the terminal voltage would be made:

$$\begin{aligned} VT &\le 0.97 && \text{then } e_f = \text{maximum} \\ VT &\ge 1.03 && \text{then } e_f = \text{minimum} \\ VT &= 0.0 && \text{then } e_f = 1.5 \end{aligned}$$

If these tests fail, i.e. VT is in between .97 and 1.03 then the excitation voltage, $e_f$, would be equal to the field current, $i_f$, divided by the terminal voltage squared:

$$e_f[(k+1)T] = i_f[kT] / (VT[kT])^2$$

The test for zero terminal voltage is to insure that under short circuit conditions there is a field current maintained so that the short circuit current will last long enough to trip the circuit breakers about the short, [10]. A comparison between this proposed digital AVR and the present controller can be found in section four.

## 3.2 THE PROPOSED DIGITAL SPEED CONTROLLER

A digital governor could also be found by implementing the present controller in a digital scheme. This digital governor would require a digital tachometer or frequency counter and a digital position indicator for the throttle. The linearized model of the current governor is:

$$\dot{VP} = (DVP - VP + (1-\omega)*K_h)/T_h \qquad 2.4.1$$

$$\dot{DVP} = (VP - DVP)/T_1 \qquad 2.4.2$$

These equations would convert to the following z transform transfer equation:

$$\frac{VP(z)}{(1-\omega)(z)} = \frac{\frac{K_h}{T_h}z^2 - \left(\frac{K_h T_1}{T_h(T_h+T_1)} + \frac{K_h T_h e^{-\frac{T\,T_h\,T_1}{T_h+T_1}}}{T_h(T_h+T_1)}\right)z}{z^2 - \left(1 - e^{-\frac{T\,T_h\,T_1}{T_h+T_1}}\right)z + e^{-\frac{T\,T_h\,T_1}{T_h+T_1}}} \qquad 3.2.1$$

In difference equation form

$$VP[(k+1)T] = (1+e^{-T\beta})VP[kT] - e^{-T\beta}VP[(k-1)T] + {}^{K_h}/T_h(1-\omega)[(k+1)T]$$

$$- \left( \frac{K_h T_1}{T_h(T_h+T_1)} + \frac{K_h T_h e^{-T\beta}}{T_h(T_h+T_1)} \right) (1-\omega)[kT] \qquad 3.2.2$$

A much simpler digital governor can be found.

The present governor depends on a speed change of fixed magnitude before the throttle reacts to a change in generator load. Since the inerita constant of the turbogenerator is so large, this governor reacts sluggishly to load changes. The result is that the turbogenerator is allowed to oscillate slowly about the desired frequency. A digital governor could easily improve this action by altering the turbine power before the speed has a chance to change. This proposed digital governor would compute the power output of the generator and use this information to alter the turbines power. This would greatly reduce the speed fluctuations. The easiest method of arriving at generator power is the instantaneous generator voltage times current. To complete the governor an actual speed signal must be used to maintain the exact speed. Thus an error signal can be added to the generator power to return the system to rated speed. However, when an error signal is added, the speed will again fluctuate. To prevent this, information about the change of speed of the system can be subtracted from the error signal. In this manner the

speed can be returned to rated value and not oscillate. The proposed governor would use generator power, $P_{ele}$, and system speed, $\omega$, to control throttle position, VP:

$$VP[(k+1)T] = \{P_{ele}[kT] + .1 + ({}^{5}/_{T}-1)\omega[kT] - {}^{5}/_{T}\omega[(k-1)T]\}/T_{ch}$$

$$P_{ele}[kT] = \sum_{\phi} V[kT]*i[kT]$$

A comparison between the proposed digital governor and the present governor can be found in Section four.

# IV THE RESULTS OF THE SIMULATIONS

In this section the models and controllers will be compared and evaluated. First the models will be compared to the actual acceptance test results, and to each other. Then the proposed digital controller will be compared to the present controller. Finally the remaining test results will be presented. Most of the information will be presented graphically as the responses of the models to various imposed loads.

## 4.1 TESTS ON THE MODELS

The generator acceptance tests provide information on the actual generator response to three phase short circuit and to no load to full load, full volt-amperes load. The full load was an induction motor with its rotor locked. It provided a per unit impedence of .5887 + j1.691. The generators response may be seen in figures 4.1.1 and 4.1.2. The tests were on the generator alone and no turbogenerator test results were available. The frequency responses therefore are based on the design specifications. In figures 4.1.3 and 4.1.4 the dq0 generator model was simulated under the same load conditions as the acceptance tests. Under the no load to full load the dq0 model produced smoother results but they were similar to the test response. Table 4.1.1 provides a summary of the responses.

These tests were repeated and the results are illustrated in figures 4.1.5 and 4.1.6 with the three phase model providing the responses. Again the results are similar. Because of the amount of time required to simulate this model, the responses are for shorter periods of time. The accuracy of the model is apparent from these results.

Comparison of the two models to determine which is more accurate is difficult. Both models perform adequately under the information available for these tests. The determining factor in choosing which model to use should be based on the advantages of the specific model to simulate the conditions which will be imposed. The dq0 model has advantages in speed of execution and memory required. The dq0 model requires on the average 0.066 CPU seconds per cycle to simulate average load conditions whereas, the three phase model required 1.6 CPU seconds to simulate the same load. Also the dq0 model required about two thirds the memory that the three phase model required. Under other load conditions the difference in execution time can be reduced but the three phase model always requires more time.

## 4.2 TESTS ON THE PROPOSED CONTROLLERS

Now the simulation of the proposed digital controllers will be compared to the model of the present controllers. Because of its higher speed of execution the dq0 model was used throughout this section. First the frequency response

FIGURE 4.1.1

GENERATOR 3 PHASE SHORT CIRCUIT TEST

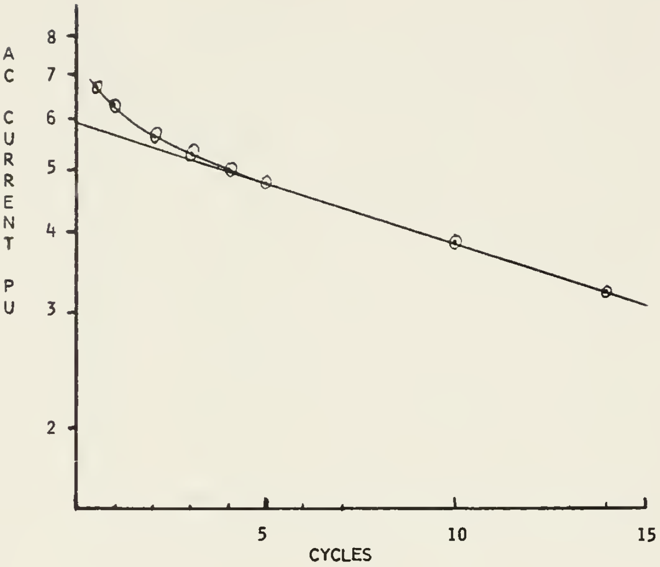

FIGURE 4.1.2

GENERATOR NO LOAD TO FULL LOAD TEST

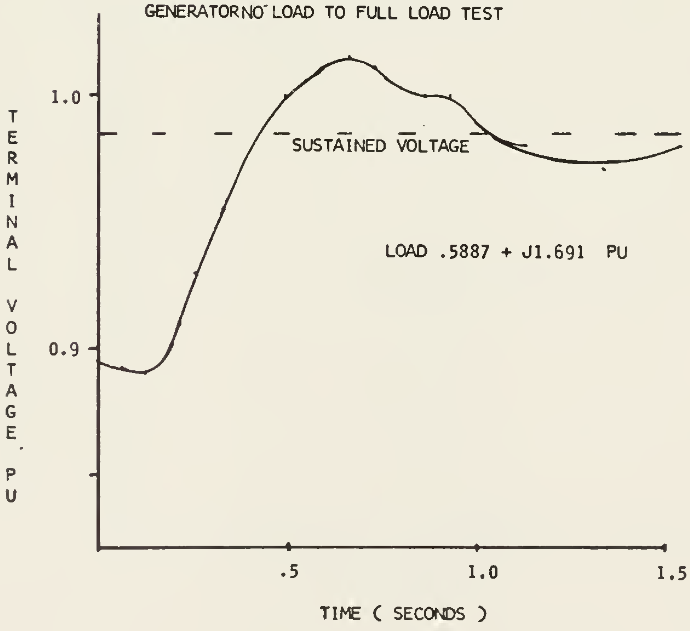

FIGURE 4.1.3
DQ0 GENERATOR MODEL 3 PHASE SHORT CIRCUIT TEST

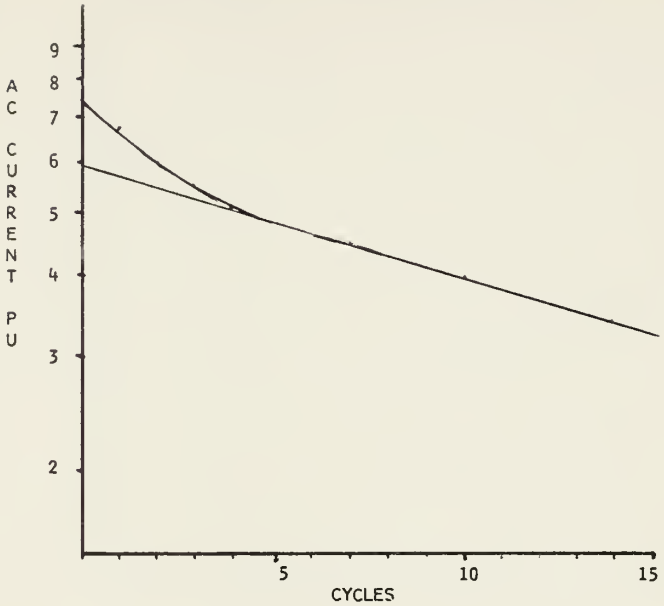

FIGURE 4.1.4

DQO GENERATOR MODEL NO LOAD TO FULL LOAD TEST

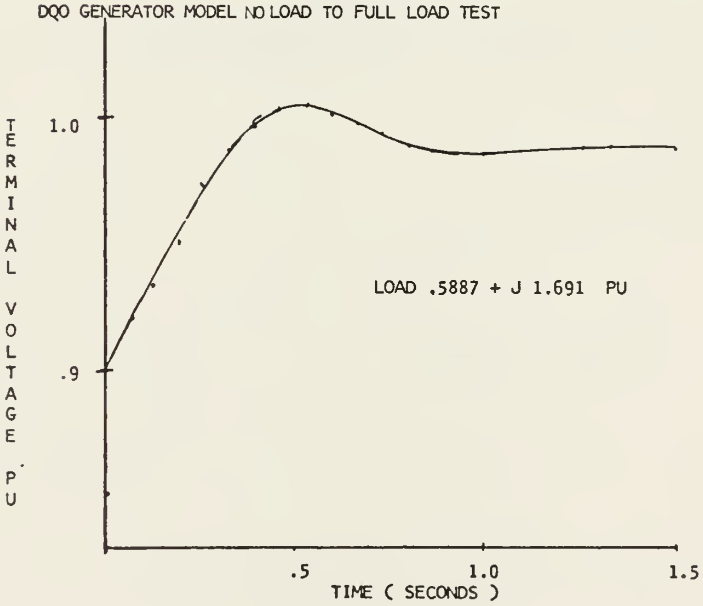

FIGURE 4.1.5

THREE PHASE GENERATOR MODEL SHORT CIRCUIT TEST

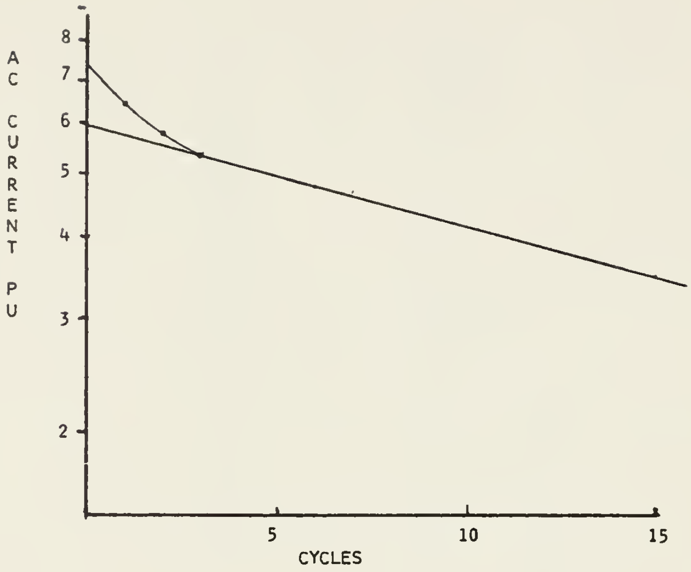

FIGURE 4.1.6

THREE PHASE GENERATOR MODEL NO LOAD TO FULL LOAD TEST

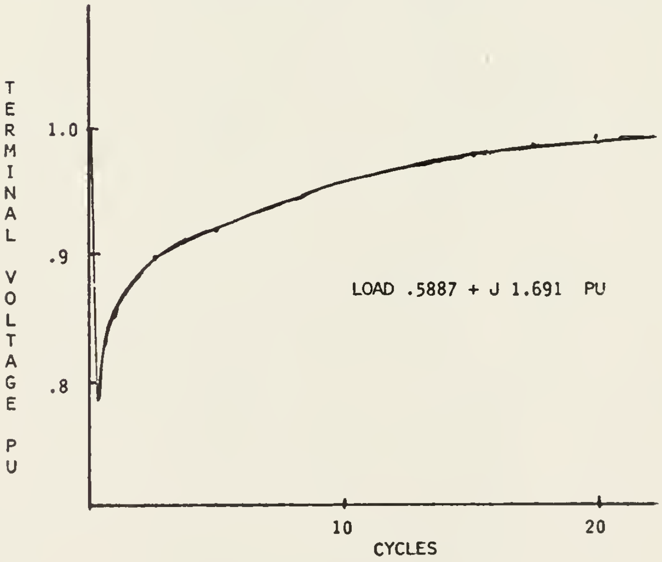

|  | Short Circuit Test |  |  |  | No load to full Load |  |
|---|---|---|---|---|---|---|
| system | $x'_d$ | $x''_d$ | $T'_d$ | $T''_d$ | Rise Time | Settlig Time |
| generator | .167 | .135 | .314 | .0185 | .5 | .71 |
| dq0 model | .161 | .133 | .273 | .023 | .333 | .70 |
| three phase model | .167 | .135 | .293 | .020 | .333 | xxx |

Table 4.2.1

of the turbogenerator to the no load to full load, locked rotor induction motor, must be established. The design specifications is for the turbogenerator to remain within 6% of rated value, 4% for normal load fluctuation, and return to within two percent of rated speed within two seconds. Figure 4.2.1 is the simulated response of the system frequency under this load.

In figure 4.2.2 and 4.2.3 the dq0 generator model is controlled by the proposed digital controller. Again the voltage dip is .89, however the rise time and settling time are greatly reduced. The frequency response is even better. Here the variation is one third as great as the actual controller. The proposed digital controller also returns the frequency to exactly rated value, rather than to within two percent of rated value. The proposed governor requires about three seconds to return to rated speed.

To further test the proposed digital controller an even larger load fluctuation was simulated. The locked rotor induction motor provided full volt-amperes for the generator but the actual power required was only about forty percent of the available power. In this test both the volt-amperes and the power required were a maximum. The simulated load was .8 + j .6 per unit. The simulated responses under the present controller are shown in figures 4.2.4 and 4.2.5. The same load conditions were repeated

FIGURE 4.2.I

DQO GENERATOR MODEL NO LOAD TO FULL LOAD

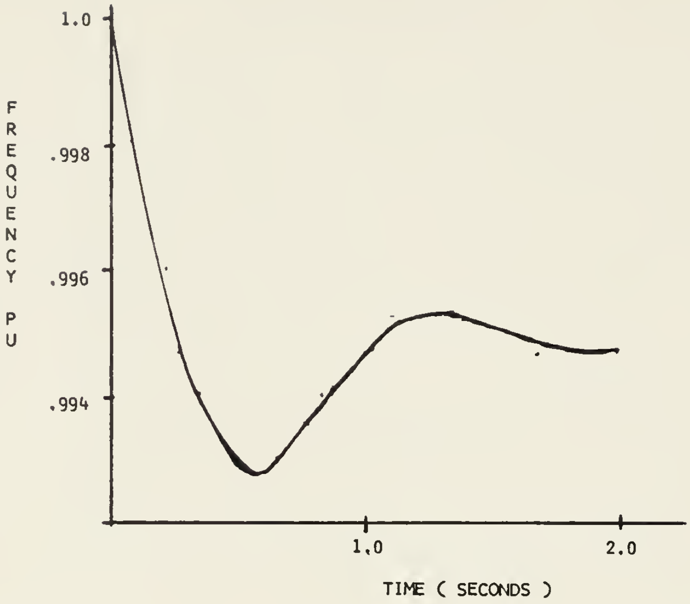

FIGURE 4.2.2

DQO GENERATOR MODEL NO LOAD TO FULL LOAD

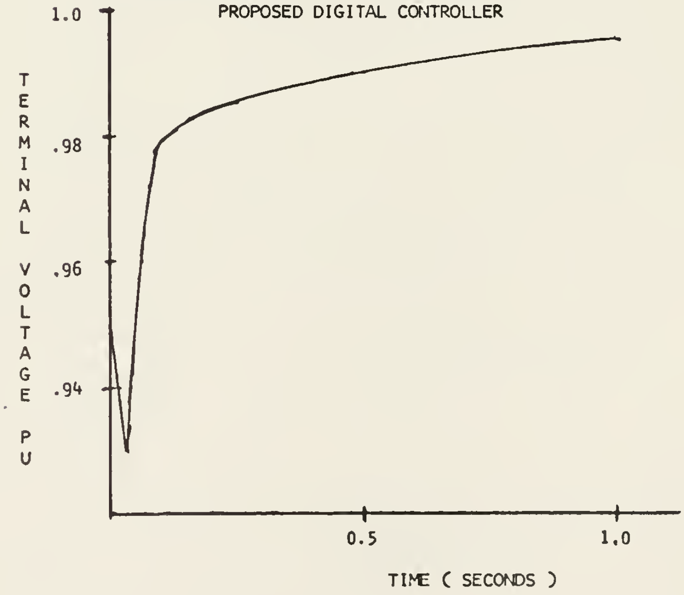

FIGURE 4.2.3

DQO GENERATOR MODEL NO LOAD TO FULL LOAD

PROPOSED DIGITAL CONTROLLER

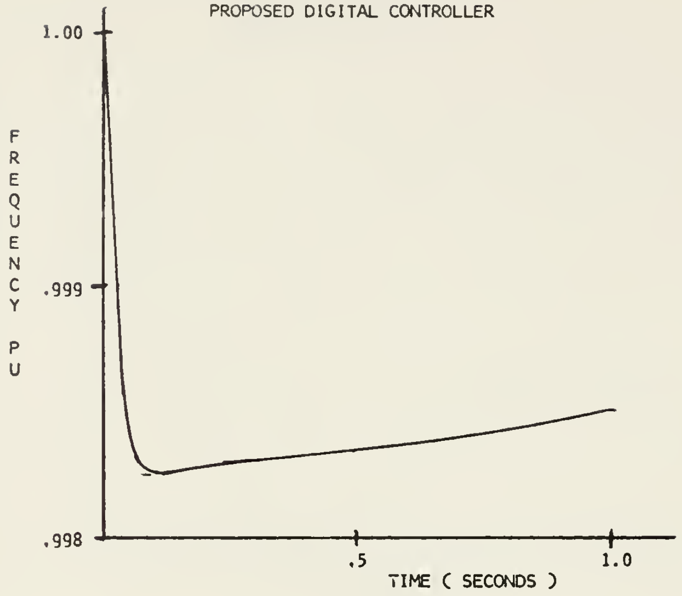

FIGURE 4.2.4

DQO GENERATOR MODEL NO LOAD TO FULL LOAD

PRESENT CONTROLLER

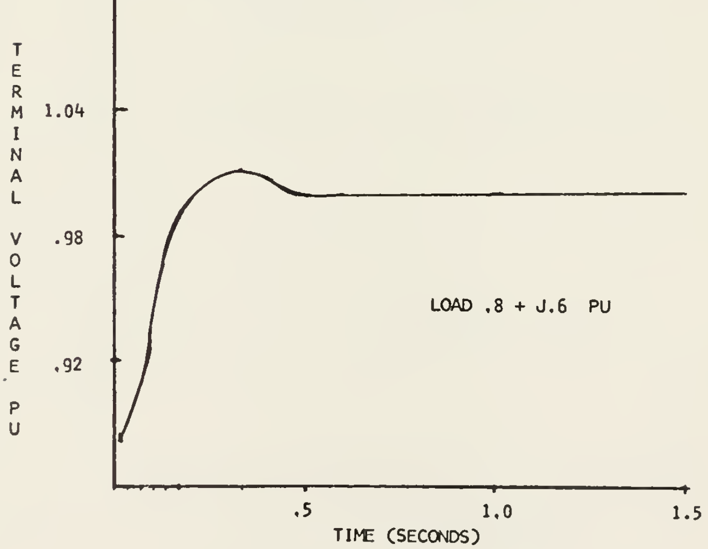

FIGURE 4.2.5

DQO GENERATOR MODEL NO LOAD TO FULL LOAD

PRESENT CONTROLLER

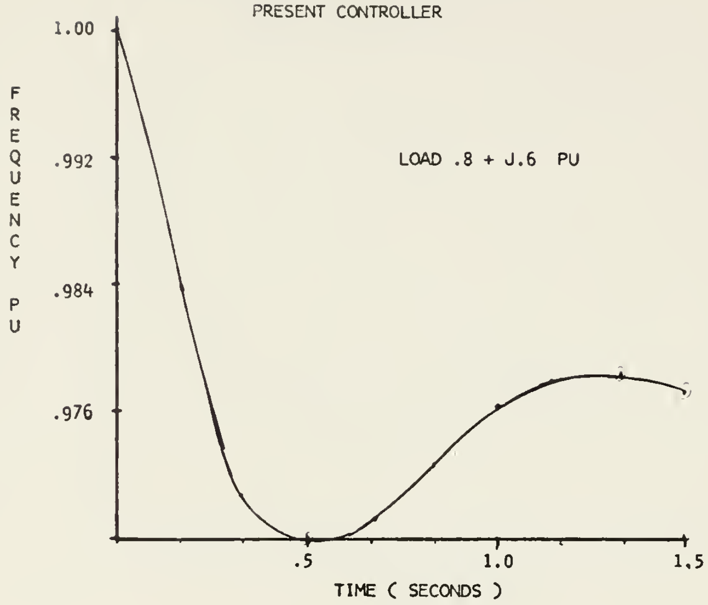

FIGURE 4.2.6

DQO GENERATOR MODEL NO LOAD TO FULL LOAD

PROPOSED DIGITAL CONTROLLER

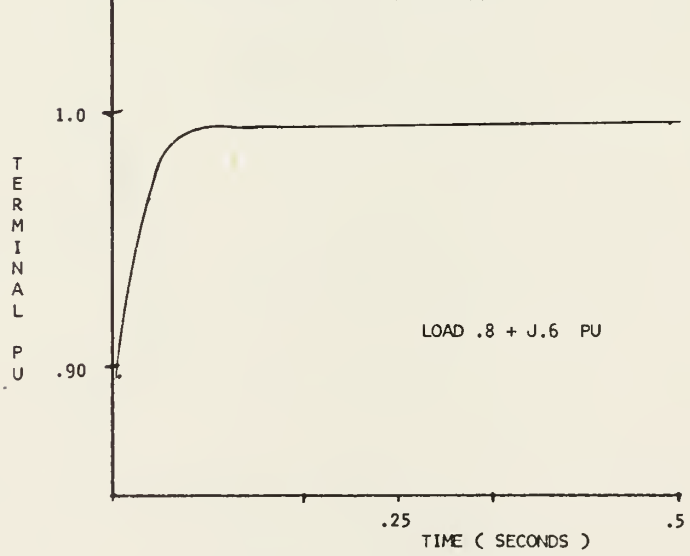

FIGURE 4.2.7

DQO GENERATOR MODEL NO LOAD TO FULL LOAD

PROPOSED DIGITAL CONTROLLER

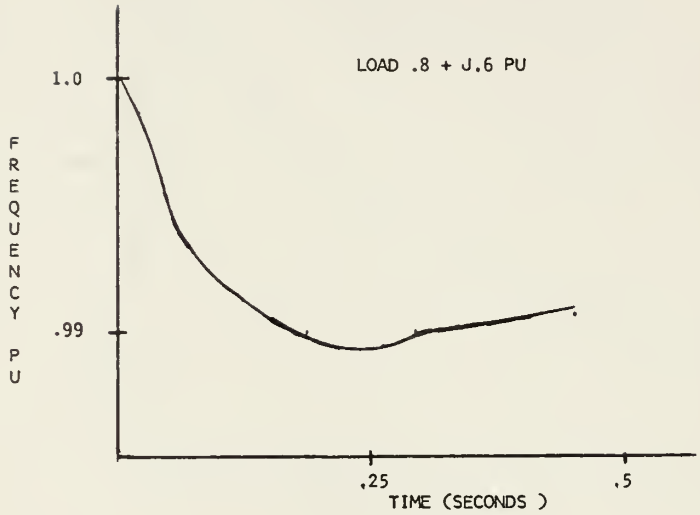

FIGURE 4.2.8

DQO GENERATOR MODEL FULL LOAD TO MOTOR LOAD

PROPOSED DIGITAL CONTROLLER

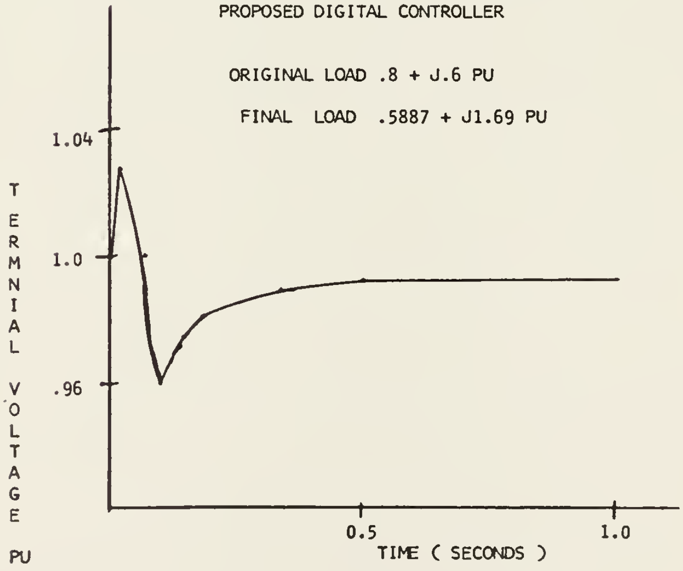

FIGURE 4.2.9

DQO GENERATOR MODEL FULL LOAD TO MOTOR LOAD

PROPOSED DIGITAL CONTROLLER

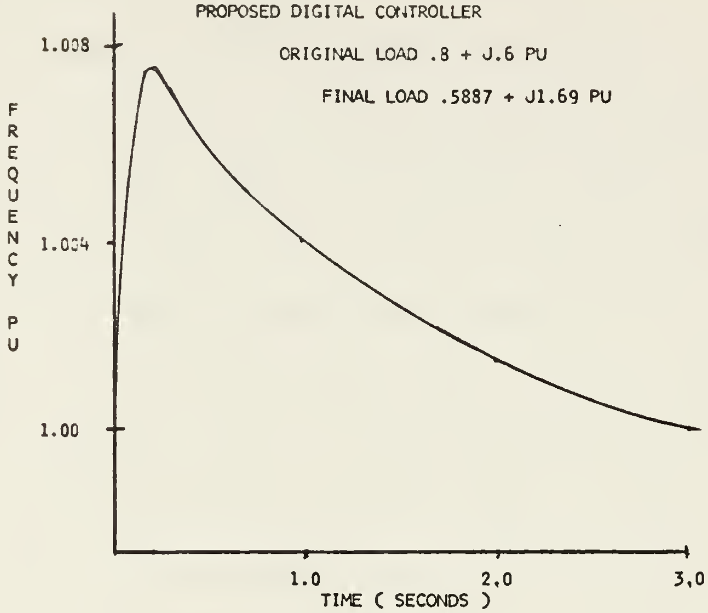

ORIGINAL LOAD .8 + J.6 PU

FINAL LOAD .5887 + J1.69 PU

with the proposed digital controller in figure 4.2.6 and 4.2.7. The proposed digital controller was faster in its response to load changes.

Finally to insure that the proposed digital controller worked completely the controller was tested under a decrease in load: from a full power load the locked rotor induction motor load. These test results, figures 4.2.8 and 4.2.9, were important because the transients induced in the field coil make the proposed AVR overshoot the correct value. The proposed digital controller still performed well on this test. This simulation was carried far enough to be able to see the governor return the system to rated speed.

Throughout this and all other tests the simple proposed digital controller out performed the actual machine controllers.

## 4.3 TESTS ON SAMPLING RATE

The rapidity at which the proposed digital controller must reestimate the correct throttle position and excitation voltage greatly affect the cost of the proposed controller. For the digital automatic voltage regulator the full resistive load is the worst case. Under this load the generator responds faster than any other condition. By simulation under full resistive load if the digital AVR reestimates a new required excitation voltage every 0.4 cycles, a new estimate of

the required excitation voltage can be calculated before the terminal voltage can overshoot its rated value. Thus, the field current does not overshoot the predicted value even when the terminal voltage is below the value forcing the excitor into its limits.

Under other load conditions, especially high inductive loads the period between estimates can be considerably slower. Under the locked rotor induction motor load, the proposed digital AVR would only have to reestimate the required excitation voltage once every 2.3 cycles to prevent the terminal voltage from oscillating. For the load .8 + j.6 pu. the AVR must reestimate the required excitation voltage at least once a cycle to prevent the terminal voltage from oscillating. To insure that the AVR does not cause oscillation of the terminal voltage a sampling rate of 120 times per second is recommended. This rate would adequately handle any load condition.

The proposed digital governor does not have such a critical sampling rate. The sampling rate of the governor would depend more on the frequency of the load changes. The slower the sampling rate the larger would be the frequency fluctuations. A rate of about thirty times a second or once every two cycles is recommended to allow this proposed digital governor to out perform the present governor.

## 4.4 POSSIBLE FAULTS IN THE PROPOSED CONTROLLERS

Another problem that might arise with the proposed digital AVR could result from not correctly knowing the field resistance. This would cause the AVR to incorrectly estimate the required excitation voltage. This would result in either an oscillation if the field resistance were lower than expected or in the AVR's response time decreasing significantly if the resistance were larger than expected. The error in the value of the field resistance would have to be considerable to noticeably affect the operation of the proposed AVR. If the terminal voltage did tend to oscillate slightly and this was determined to be the cause, the AVR could be altered to use information about the rate of change of field current to improve its estimate of required excitation voltage and eliminate the oscillation.

# V CONCLUSIONS

The objective of this thesis was to compare the three phase generator model to the dq0 generator model and to find a simple digital control scheme which would meet the design specifications of the shipboard turbogenerator.

The two computer models, the three phase and the dq0, were found to agree completely in all respects. The three phase model would require more computer storage and execution time than the dq0 model. However, the three phase model would simulate more complicated load and saturation conditions than would the dq0 model.

This thesis showed that if complicated load and saturation conditions were to be simulated the three phase model would be beneficial. If balanced load and saturation conditions were to be simulated the dq0 model would result in considerable savings in time. Both models were satisfactory in simulating the different controllers.

A simple digital controller has been proposed which by using information easily obtained digitally, but difficult to obtain by analogue means, has significantly improved the performance of the turbogenerator model to load changes.

This investigation should be continued to further test the affects of saturation and a multi-machine environment. After these tests were satisfactorily passed the supreme test would be to build and install such a digital controller.

## BIBLIOGRAPHY

1. Blackman, Raymond V. B., (ed.) *Jane's Fighting ships 1971/1972 Edition*, London: S. Low Marston & Co., Ltd., 1972.
2. U. S. Navy, *NAVSHIPS TECH MANUAL 0361-170-2002*, Change 2, April 1970, Hyattsville, MD.: Bureau of Naval Ships, 1970.
3. IEEE Committee Report, "Dynamic Models for Steam and HydroTurbines in Power System Studies", *IEEE Transactions on Power Appratus and Systems*, Vol 92 No 6, Nov/Dec 1973.
4. Concordia, Charles, *Synchronous Machines Theory and Performance*, New York: John Wiley & Sons, Inc., 1951.
5. Kimbark, Edward Wilson, *Power System Stability, Vol III, Synchronous Machines*, New York: John Wiley & Sons, Inc., 1956.
6. Dunfield, J. C., and T. H. Barton, "Effect on M.M.F. and Pereance Harmonics in Electrical Machines", *Proceedings* (Institute of Electrical Engineers, London), 1967, Vol 114 No 10.
7. Factory Test Record, Allis Chalmers Mfg., Co., Milwaukee, Wisconsin on Generator serial no. 161566.
8. Subramanian, P., and O. P. Malik, "Digital Simulation of a Synchronous Generator in Direct-Phase Quantities", *Proceeding* (Institute of Electrical Engineers, London), 1971, Vol 118 No 1.

9. IEEE Committee Report, "Computer Representation of Excitation Systems", IEEE Transactions on Power Appratus and Systems, Vol 87 No 6, 1968.

10. Miller, D. H., and A. S. Rubenstein, "Excitation Systems for Small Industrial and Commercial Generators", IEEE Transactions of Power Appratus and Systems, Vol 82 No 2, 1963.

11. Kimbark, Edward Wilson, Power System Stability, Vol I, Elements of Stability Calculations, New York: John Wiley & Sons, Inc, 1948.

12. Hammons, T. J., and D. J. Winning, "Comparisons of Synchronous Machine Models in the Study of the Transient Behavior of Electrical Power Systems", Proceedings (Institute of Electrical Engineers, London), Vol 118 No 10, October 1971.

13. Carr, Laurence H. A., The Testing of Electrical Machines, London: MacDonald & Co. 1960

14. Dandeno, Paul L., Kundur Prabhashankar, and Richard P. Schulz, "Recent Trends and Progress in Synchronous Machine Modelling in Electric Utility Industry", Proceedings of the IEEE, Vol 62 No 7 July 1974.

15. Smith, Ralph J., Circuits, Devices, and Systems, New York: John Wiley & Sons, Inc., 1967.

# APPENDIX

## A.1 Calculation of Inertia Constant

To calculate the inertia constant, H, the moment of inertia of the system was required, Figure 9 is a basic drawing of the rotating parts showing size and weight of each. By assuming constant density throughout each piece and neglecting light projections, such as the coupling and actual turbine blades, the moment of inertia was computed by integrating

$$WR^2 = \int_0^{\ell} \int_0^{2\pi} \int_0^{r} \rho \, r^3 \, dr d\theta dl$$

or since all parts are cylinderical $WR^2 = \pi r^4/_2$ under constant density.

The moment of inertia of the major parts is:

| | | | |
|---|---|---|---|
| turbine | 89.08 | ft lbs | at 10009 RPM |
| pinion | .89 | ft lbs | at 10009 RPM |
| gear | 81843.8 | ft lbs | at 1200 RPM |
| generator | 8680.8 | ft lbs | at 1200 RPM |

The inertia constant is the moment of inertia converted to kinetic energy terms and put in the per unit system. Thus converting to megajoule-seconds per radian and then dividing by the apparent power, volt-amperes, the inertia constant is, [11]:

$$H = 24.29 \frac{\text{joule seconds}}{\text{volt ampere}} \text{ (actually dimensionless)}$$

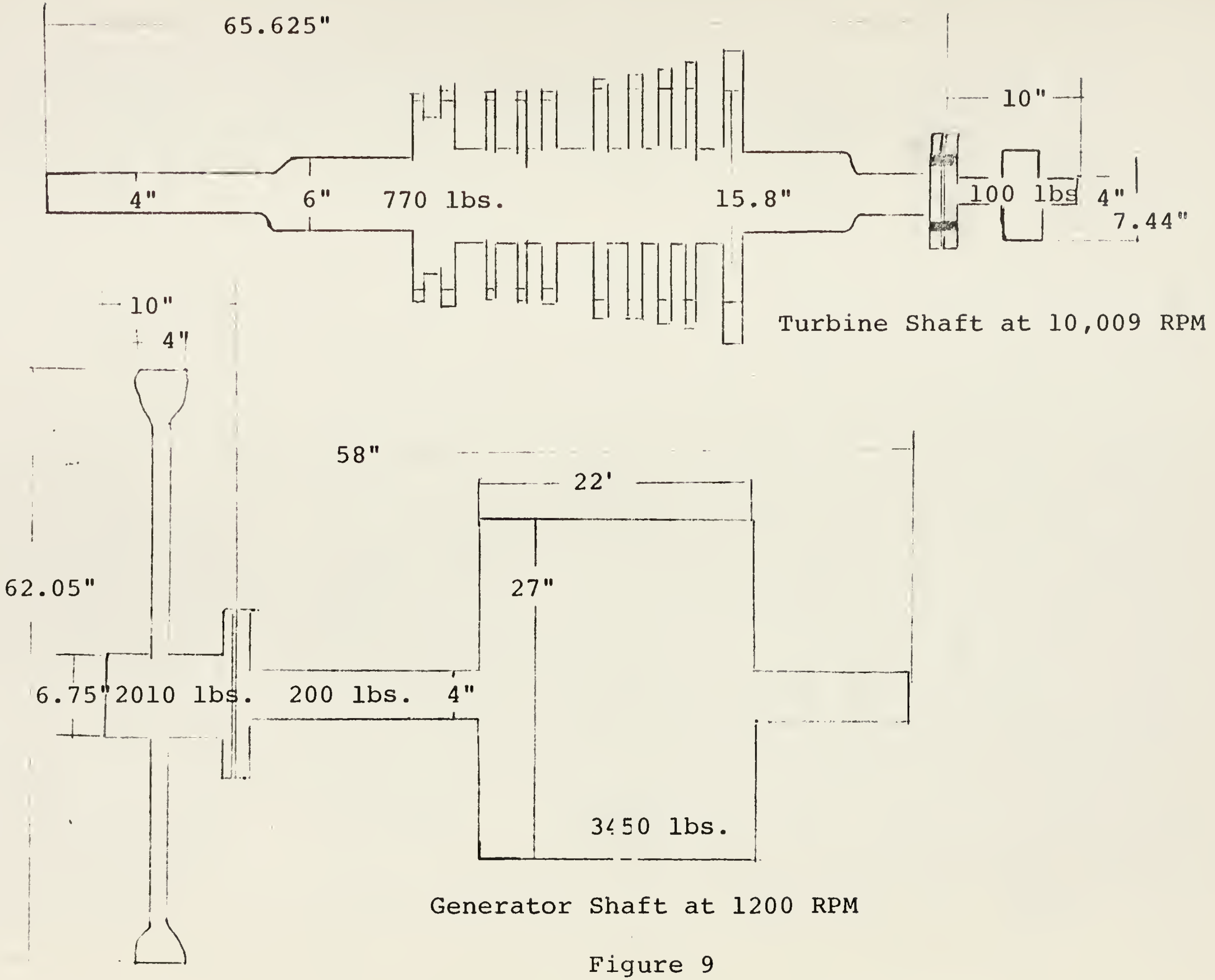
65.625"
10"
4"
6"
770 lbs.
15.8"
100 lbs
4"
7.44"
10"
4"
58"
22'
62.05"
27"
6.75"
2010 lbs.
200 lbs.
4"
3450 lbs.

Turbine Shaft at 10,009 RPM

Generator Shaft at 1200 RPM

Figure 9

## A.2 Calculation of Generator Constants

The short circuit tests, [7], provided the information to calculate the machine constants. The short circuit provided values for direct axis reactance, $x_d$, direct axis transient reactance, $x_d'$, direct axis subtransient reactance, $x_d''$, and external reactance, $x_2$. Also given were the phase and rotor resistances and the voltage dip for an initial load. From this the fact that $x_2 \neq x_d''$ would indicate that the generator was a salient pole machine which was previously known. The subtansient quadrature axis reactance was calculated from $x_2$ and $x_d''$ by $x_2 = \sqrt{x_d'' \, x_q''}$. The external reactance is an approximate time average of the subtransient reactances. The quadrature axis reactance was more difficult. The only information available was the voltage dip, however this depends mainly on the direct axis transient reactance. This was used as an approximation for the value of the quadrature axis reactance, $x_q$. The zero axis reactance, $x_0$, which was never used since only balanced loads were simulated was derived from $x_2$, $x_d''$, and $x_q''$.

With the machine time constants the remaining constants followed easily. The direct axis to field axis mutual inductance was assumed to be only slightly less than the direct axis reactance due to the leakage of lines of flux. The same leakage was assumed for the quadrature axis. Thus

$$x'_d = x_d - \frac{L^2_{df}}{L_f} \qquad 74$$

$$x''_d = x_d - \frac{L_{kd}L^2_{df} - 2L_{fkd}L_{dkd}L_{df} + L_fL^2_{dkd}}{L_{kd}L_f - L^2_{fkd}} \qquad 123$$

$$x''_q = x_q - \frac{L^2_{qkq}}{L_{kq}} \qquad 124$$

The field time constant, $T'_d$ , by

$$T'_d = \frac{L_f \; x'_d}{R_f \; x_d} \qquad 139$$

The field transient time constant, $T''_d$ , by

$$T''_d = \frac{L_{kd} - L^2_{fkd}/L_f}{R_{kd}} \quad \frac{x''_d}{x'_d} \qquad 140$$

The quadrature axis time constant had to be completely approximated by a table in [4], chosing a value for a machine which was similar in the known constants.

$$T''_q = \frac{L_{kq} - L^2_{qkq}/L_q}{R_{kq}} \qquad 138$$

The three phase constants are two thirds of these values except for the stator values. These phase values are determined by

$$x_d = L_{aa0} + L_{ab0} + {}^{3}/_{2} L_{aa2} \tag{25}$$

$$x_q = L_{aa0} + L_{ab0} - {}^{3}/_{2} L_{aa2} \tag{26}$$

$$x_0 = L_{aa0} - 2\, L_{ab0} \tag{27}$$

These equations are directly from [4], and [5], the equation numbers are the numbers assigned in [4].

## Machine Constants

Measured Values (again all values are in per unit )

$x_d = 1.5$

$x'_d = 0.167$

$x''_d = 0.135$

$x_2 = 0.23$

$T'_d = 1078$ radians

$T''_d = 7.78$ radians

Voltage Dip = .89

Computed Values

| dq0 Model | Three Phase Model |
|---|---|
| $L_d = 1.5$ | $L_{aa0} = 0.936$ |
| $L_q = 1.217$ | $L_{ab0} = 0.4225$ |
| $L_0 = 0.091$ | $L_{aa2} = 0.0943$ |
| $L_{df} = 1.4$ | $L_{af} = .933$ |
| $L_{dkd} = 1.4$ | $L_{akd} = .933$ |
| $L_{qkq} = 1.14$ | $L_{akq} = .76$ |
| $L_f = 1.47$ | $L_f = .98$ |
| $L_{kd} = 1.47$ | $L_{kd} = .98$ |
| $L_{kq} = 1.217$ | $L_{kq} = .8113$ |
| $L_{fkd} = 1.408$ | $L_{fkd} = .9387$ |

$R_f = 0.0013725$

$R_{kd} = 0.01716$

$R_{kq} = 0.143$

$R_a = 0.018$

$R_f = 0.000915$

$R_{kd} = 0.01142$

$R_{kq} = 0.0953$

$R_a = 0.018$

# VITA

NAME: William Lloyd Hatcher III

Lieutenant Junior Grade

United States Navy

DATE OF BIRTH: 24 JUNE 1949

PLACE OF BIRTH: Jacksonville, Florida

COLLEGES AND DEGREES: U. S. Naval Academy

Annapolis, Maryland

B.S.S.E.

155658
Thesis
H3175 Hatcher
Digital control of
a shipboard turbogenerator.

[illegible]74 DISPLAY

155658
Thesis
H3175 Hatcher
Digital control of
a shipboard turbogenerator.

thesH3175
Digital control of a shipboard turbogene
3 2768 001 01828 6
DUDLEY KNOX LIBRARY